1   **Global inorganic nitrate production mechanisms:**

2   **Comparison of a global model with nitrate isotope**

3   **observations**

4

5   Becky Alexander[1], Tomás Sherwen[2,3], Christopher D. Holmes[4], Jenny A. Fisher[5], Qianjie

6   Chen[1,6], Mat J. Evans[2,3], Prasad Kasibhatla[7]

7

8   [1]Department of Atmospheric Sciences, University of Washington, Seattle, WA 98195, USA

9   [2]Wolfson Atmospheric Chemistry Laboratories, Department of Chemistry, University of York, York YO10 5DD, UK

10   [3]National Center for Atmospheric Science, University of York, York YO10 5DD, UK

11   [4]Department of Earth, Ocean and Atmospheric Science, Florida State University, Tallahassee, FL 32306, USA

12   [5]Centre for Atmospheric Chemistry, University of Wollongong, Wollongong, New South Wales 2522, Australia

13   [6]Now at Department of Chemistry, University of Michigan, Ann Arbor, MI 48109, USA

14   [7]Nicholas School of the Environment, Duke University, Durham, NC 27708, USA

15

16   Correspondence to: Becky Alexander (beckya@uw.edu)

17

18   **Abstract.** The formation of inorganic nitrate is the main sink for nitrogen oxides (NO_x = NO + NO_2). Due to the

19   importance of NO_x for the formation of tropospheric oxidants such as the hydroxyl radical (OH) and ozone,

20   understanding the mechanisms and rates of nitrate formation is paramount for our ability to predict the atmospheric

21   lifetimes of most reduced trace gases in the atmosphere. The oxygen isotopic composition of nitrate ($\Delta^{17}O$(nitrate)) is

22   determined by the relative importance of NO_x sinks, and thus can provide an observational constraint for NO_x

23   chemistry. Until recently, the ability to utilize $\Delta^{17}O$(nitrate) observations for this purpose was hindered by our lack

24   of knowledge about the oxygen isotopic composition of ozone ($\Delta^{17}O(O_3)$). Recent and spatially widespread

25   observations of $\Delta^{17}O(O_3)$ have greatly reduced this uncertainty, and allow for an updated comparison of modeled and

Atmospheric
Chemistry
and Physics
Discussions

1   observed $\Delta^{17}O$(nitrate) and a reassessment of modeled nitrate formation pathways. Model updates based on recent

2   laboratory studies of heterogeneous reactions renders dinitrogen pentoxide (N_2O_5) hydrolysis as important as NO_2 +

3   OH (both 41%) for global inorganic nitrate production near the surface. All other nitrate production mechanisms

4   represent less than 6% of global nitrate production near the surface, but can be dominant locally. Updated reaction

5   rates for aerosol uptake of NO_2 result in significant reduction of nitrate and nitrous acid (HONO) formed through this

6   pathway in the model, and render NO_2 hydrolysis a negligible pathway for nitrate formation globally. Although

7   photolysis of aerosol nitrate may have implications for NO_x, HONO and oxidant abundances, it does not significantly

8   impact the relative importance of nitrate formation pathways.   Modeled $\Delta^{17}O$(nitrate) (28.6 ± 4.5‰) compares well

9   with the average of a global compilation of observations (27.6 ± 5.0‰), giving confidence in the model's

10   representation of the relative importance of ozone versus HO_x (= OH + HO_2 + RO_2) in NO_x cycling and nitrate

11   formation.

12

13   **1. Introduction**

14

15   Nitrogen oxides (NO_x = NO + NO_2) are a critical ingredient for the formation of tropospheric ozone (O_3).

16   Tropospheric ozone is a greenhouse gas, is a major precursor for the hydroxyl radical (OH), and is considered an air

17   pollutant due to its negative impacts on human health. The atmospheric lifetime of NO_x is determined by its oxidation

18   to inorganic and organic nitrate. The formation of inorganic nitrate (HNO_3(g) and particulate NO_3^-) is the dominant

19   sink for NO_x globally, while formation of organic nitrate may be significant in rural and remote continental locations

20   (Browne and Cohen, 2014). Organic nitrate as a sink for NO_x may be becoming more important in regions in North

21   America and Europe where NO_x emissions have declined (Zare et al., 2018). Uncertainties in the rate of oxidation of

22   NO_x to nitrate has been shown to represent a significant source of uncertainty for ozone and OH formation in models

23   (e.g., Newsome and Evans (2017)) , with implications for our understanding of the atmospheric lifetime of species

24   such as methane, whose main sink is reaction with OH.

25

26   NO_x is emitted to the atmosphere primarily as NO by fossil fuel and biomass/biofuel burning, soil microbes, and

27   lightning. Anthropogenic sources from fossil fuel and biofuel burning and from the application of fertilizers to soil

28   for agriculture currently dominate NO_x sources to the atmosphere (Jaeglé et al., 2005). After emission, NO is rapidly

Atmospheric
Chemistry
and Physics
Discussions

1   oxidized to NO_2 by ozone (O_3), peroxy (HO_2) and hydroperoxy radicals (RO_2), and halogen oxides (e.g., BrO). During

2   the daytime, NO_2 is rapidly photolyzed to NO + O at wavelengths (λ) < 424 nm. NO_x cycling between NO and NO_2

3   proceeds several orders of magnitude faster than oxidation of NO_x to nitrate during the daytime (Michalski et al.,

4   2003).

5

6   Formation of inorganic nitrate is dominated by oxidation of NO_2 by OH during the day and by the hydrolysis of

7   dinitrogen pentoxide (N_2O_5) at night (Alexander et al., 2009). Recent implementation of reactive halogen chemistry

8   in models of tropospheric chemistry show that formation of nitrate from the hydrolysis of halogen nitrates (XNO_3,

9   where X = Br, Cl, or I) is also a sink for NO_x with implications for tropospheric ozone, OH, reactive halogens, and

10   aerosol formation (Schmidt et al., 2016;Sherwen et al., 2016;Saiz-Lopez et al., 2012;Long et al., 2014;Parrella et al.,

11   2012;von Glasow and Crutzen, 2004). Other inorganic nitrate formation pathways include hydrogen-abstraction of

12   hydrocarbons by the nitrate radical (NO_3), heterogeneous reaction of N_2O_5 with particulate chloride (Cl^-),

13   heterogeneous uptake of NO_2 and NO_3, direct oxidation of NO to HNO_3 by HO_2, and hydrolysis of organic nitrate.

14   Inorganic nitrate partitions between the gas ($HNO_3(g)$) and particle (NO_3^-) phases, with its relative partitioning

15   dependent upon aerosol abundance, aerosol liquid water content, aerosol chemical composition, and temperature.

16   Inorganic nitrate is lost from the atmosphere through wet or dry deposition to the Earth's surface with a global lifetime

17   against deposition on the order of 3-4 days (Alexander et al., 2009).

18

19   Formation of inorganic nitrate was thought to be a permanent sink for NO_x in the troposphere due to the slow

20   photolysis of nitrate compared to deposition. However, laboratory and field studies have shown that NO_3^- adsorbed

21   on surfaces is photolyzed at rates much higher than $HNO_3(g)$ (Ye et al., 2016). The photolysis of NO_3^- in snow grains

22   on ice sheets has a profound impact on the oxidizing capacity of the polar atmosphere (Domine and Shepson, 2002).

23   More recently, observations of NO_x and nitrous acid (HONO) provide evidence of photolysis of aerosol NO_3^- in the

24   marine (Reed et al., 2017;Ye et al., 2016) and continental (Ye et al., 2018;Chen et al., 2019) boundary layer, with

25   implications for ozone and OH (Kasibhatla et al., 2018).

26

27   Organic nitrates form during reaction of NO_x and NO_3 with biogenic volatile organic compounds (BVOCs) and their

28   oxidation products (organic peroxy radicals, RO_2) (Browne and Cohen, 2014;Liang et al., 1998). Products of these

Atmospheric
Chemistry
and Physics
Discussions

1   reactions include peroxy nitrates (RO_2NO_2) and alkyl and multifunctional nitrates ($RONO_2$) (O'Brien et al., 1995).

2   Peroxy nitrates are thermally unstable and decompose back to NO_x on the order of minutes to days at warm

3   temperatures. Decomposition of longer-lived peroxy nitrates such as peroxyacetyl nitrate (PAN) can provide a source

4   of NO_x to remote environments (Singh et al., 1992). The fate of $RONO_2$ is uncertain. First-generation $RONO_2$ is

5   oxidized to form second-generation $RONO_2$ species with a lifetime of about a week for the first-generation species

6   with ≥ 4 carbon atoms, and up to several weeks for species with fewer carbon atoms (e.g., days to weeks for methyl

7   nitrate) (Fisher et al., 2018). Subsequent photolysis and oxidation of second-generation $RONO_2$ species can lead to

8   the recycling of NO_x (Müller et al., 2014), although recycling efficiencies are highly uncertain (Horowitz et al.,

9   2007;Paulot et al., 2009). $RONO_2$ can also partition to the particle phase ($pRONO_2$) contributing to organic aerosol

10   formation (Xu et al., 2015). $pRONO_2$ is removed from the atmosphere by deposition to the surface, or through

11   hydrolysis to form inorganic nitrate and alcohols (Rindelaub et al., 2015;Jacobs et al., 2014).

12

13   The oxygen isotopic composition ($\Delta^{17}O = \delta^{17}O - 0.52 \times \delta^{18}O$) of nitrate is determined by the relative importance of

14   oxidants leading to nitrate formation from the oxidation of NO_x (Michalski et al., 2003). Observations of the oxygen

15   isotopic composition of nitrate ($\Delta^{17}O(nitrate)$) have been used to quantify the relative importance of different nitrate

16   formation pathways and to assess model representation of the chemistry of nitrate formation in the present day

17   (Alexander et al., 2009;Michalski et al., 2003;Costa et al., 2011;Ishino et al., 2017a;Morin et al., 2009;Morin et al.,

18   2008;Savarino et al., 2007;Kunasek et al., 2008;Savarino et al., 2013;McCabe et al., 2007;Morin et al., 2007;Hastings

19   et al., 2003;Kaiser et al., 2007;Brothers et al., 2008;Ewing et al., 2007) and in the past from nitrate archived in ice

20   cores (Sofen et al., 2014;Alexander et al., 2004;Geng et al., 2014;Geng et al., 2017). Ozone-influenced reactions in

21   NO_x oxidation lead to high $\Delta^{17}O(nitrate)$ values while HO_x-influenced reactions lead to $\Delta^{17}O(nitrate)$ near zero.

22   Oxidation by XO (where X = Br, Cl, or I) leads to $\Delta^{17}O(nitrate)$ values similar to reactions with ozone because the

23   oxygen atom in XO is derived from the reaction $X + O_3$. Therefore, $\Delta^{17}O(nitrate)$ is determined by the relative

24   importance of $O_3 + XO$ versus HO_x ($= OH + HO_2 + RO_2$) in both NO_x cycling and oxidation to nitrate. Due to rapid

25   NO_x-cycling during the daytime, NO_x achieves isotopic equilibrium and its $\Delta^{17}O$ value ($\Delta^{17}O(NO_x)$) is solely

26   determined by the relative abundance of ($O_3 + XO$) to ($HO_2 + RO_2$).

27

Atmospheric
Chemistry
and Physics
Discussions

1   The $\Delta^{17}O$ value of HO_x ($\Delta^{17}O(HO_x)$) is near zero due to isotopic exchange of OH with water vapor (Dubey et al.,

2   1997).   The $\Delta^{17}O$ value of ozone ($\Delta^{17}O(O_3)$) was until recently not well known due to uncertainties arising from

3   sampling artifacts in the earlier measurements (Johnston and Thiemens, 1997;Krankowsky et al., 1995) and has been

4   the largest source of uncertainty in quantification of nitrate formation pathways using observations of $\Delta^{17}O(nitrate)$

5   (Alexander et al., 2009). Previous modeling studies showed good agreement with observations of $\Delta^{17}O(nitrate)$ when

6   assuming $\Delta^{17}O(O_3)$ = 35‰ (Alexander et al., 2009;Michalski et al., 2003).   Recently, much more extensive

7   observations of $\Delta^{17}O(O_3)$ using a new technique (Vicars et al., 2012) show $\Delta^{17}O(O_3)$ = 26 ± 1‰ around the globe

8   (Vicars et al., 2012;Ishino et al., 2017b;Vicars and Savarino, 2014), and suggest that previous modeling studies are

9   biased low in $\Delta^{17}O(nitrate)$ (e.g., Alexander et al. (2009)), which would occur if the model underestimated the relative

10   role of ozone in NO_x chemistry. Reduction in uncertainty in the value of $\Delta^{17}O(O_3)$ enables improved interpretation of

11   $\Delta^{17}O(nitrate)$ as an observational constraint for the relative importance of nitrate formation pathways in the

12   atmosphere. Here, we examine the relative contribution of each nitrate formation pathway in a global chemical

13   transport model and compare the model with observations of $\Delta^{17}O(nitrate)$ from around the world.

14

15   **2. Methods**

16

17   We use the GEOS-Chem global chemical transport model version 12.0.0 driven by assimilated meteorology from the

18   MERRA-2 reanalysis product with a native resolution of 0.5° x 0.625° and 72 vertical levels from the surface up to

19   the 0.01 hPa pressure level. For computational expediency, the horizontal and vertical resolution were downgraded

20   to 4° x 5° and 47 vertical levels.   GEOS-Chem was originally described in Bey et al. (2001) and includes coupled

21   HO_x-NO_x-VOC-ozone-halogen-aerosol tropospheric chemistry as described in Sherwen et al. (2016) and Sherwen et

22   al. (2017) and organic nitrate chemistry as described in Fisher et al. (2016). Aerosols interact with gas-phase chemistry

23   through the effect of aerosol extinction on photolysis rates (Martin et al., 2003) and heterogeneous chemistry (Jacob,

24   2000). The model calculates deposition for both gas species and aerosols (Liu et al., 2001;Zhang et al., 2001;Wang

25   et al., 1998).

26

27   Global anthropogenic emissions, including NO_x, are from the Community Emissions Data System (CEDS) inventory

28   from 1950 – 2014 C.E. (Hoesly et al., 2018a). The CEDS global emissions inventory is overwritten by regional

Atmospheric
Chemistry
and Physics
Discussions

1 anthropogenic emissions inventories in the U.S. (EPA/NE11), Canada (CAC), Europe (EMEP), and Asia (MIX (Li et

2 al., 2017)). Global shipping emissions are from the International Comprehensive Ocean-Atmosphere Data Set

3 (ICOADS), which was implemented into GEOS-Chem as described in Lee et al. (2011). NO_x emissions from ships

4 are processed using the PARANOX module described in Vinken et al. (2011) and Holmes et al. (2014) to account for

5 non-linear, in-plume ozone and HNO_3 production. Lightning NO_x emissions match the OTD/LIS satellite

6 climatological observations of lightning flashes as described by Murray et al. (2012). Emissions from open fires are

7 from the Global Fire Emissions Database (GFED4.1). Biogenic soil NO_x emissions are described in Hudman et al.

8 (2012). Aircraft emissions are from the Aviation Emissions Inventory Code (AEIC) (Stettler et al., 2011).

9

10 Chemical processes leading to nitrate formation in GEOS-Chem have expanded since the previous work of Alexander

11 et al. (2009). Figure 1 summarizes the formation of inorganic nitrate in the current model. In the model, NO is

12 oxidized by O_3, HO_2, RO_2 and halogen oxides (XO = BrO, ClO, IO, and OIO) to form NO_2. NO_2 can form HNO_3

13 directly from its reaction with OH and HO_2 and through hydrolysis on aerosol surfaces. NO_2 can react with XO to

14 form halogen nitrates ($BrNO_3$, $ClNO_3$, and INO_3), which can then form HNO_3 upon hydrolysis (as described in

15 Sherwen et al. (2016)). NO_2 can also react with O_3 to form NO_3, which can then react with NO_2, hydrocarbons (HC),

16 and the biogenic VOCs monoterpenes (MTN) and isoprene (ISOP). Reaction of NO_3 with NO_2 forms N_2O_5, which

17 can subsequently hydrolyze or react with Cl^- in aerosol to form HNO_3. Reaction of NO_3 with HC forms HNO_3 via

18 hydrogen abstraction. Reactions of NO_3 are only important at night due to its short lifetime against photolysis.

19 Formation of organic nitrate ($RONO_2$) was recently updated in the model as described in Fisher et al. (2016). Reaction

20 of NO_3 with MTN and ISOP can form $RONO_2$. $RONO_2$ also forms from the reaction of NO with RO_2 derived from

21 OH oxidation of BVOCs. $RONO_2$ hydrolyzes to form HNO_3 on a timescale of 1 hour. Inorganic nitrate partitions

22 between the gas ($HNO_3(g)$) and particle (NO_3^-) phase according to local thermodynamic equilibrium as calculated in

23 the ISORROPIA-II aerosol thermodynamic module (Fountoukis and Nenes, 2007). $HNO_3(g)$ and NO_3^- are mainly

24 lost from the atmosphere via wet and dry deposition to the surface.

25

26 In the "standard" model, hydrolysis of N_2O_5, NO_3 ($\gamma_{NO3} = 1 \times 10^{-3}$), and NO_2 ($\gamma_{NO2} = 1 \times 10^{-4}$) occur on aerosol surfaces

27 only. Uptake and hydrolysis of N_2O_5 on aerosol surfaces depends on the chemical composition of aerosols,

28 temperature, and humidity as described in Evans and Jacob (2005). Recently, Holmes et al. (2019) updated the

Atmospheric
Chemistry
and Physics
Discussions

1   reaction probabilities of the NO_2 and NO_3 heterogeneous reactions in the model to depend on aerosol chemical

2   composition and relative humidity. Holmes et al. (2019) also updated the N_2O_5 reaction probability to additionally

3   depend on the H_2O and NO_3^- concentrations in aerosol (Bertram and Thornton, 2009). In addition to these updates

4   for hydrolysis on aerosol, Holmes et al. (2019) included the uptake and hydrolysis of N_2O_5, NO_2, and NO_3 in cloud

5   water and ice limited by cloud entrainment rates. We incorporate these updates from Holmes et al. (2019) into the

6   "cloud chemistry" model to examine the impacts on global nitrate production mechanisms. We consider the "cloud

7   chemistry" model as state-of-the science, and as such we focus on the results of this particular simulation. Additional

8   model sensitivity studies are also performed and examined relative to the "standard" model simulation. These

9   additional sensitivity simulations are described in Section 4.

10

11    $\Delta^{17}O$(nitrate) is calculated in the model using monthly-mean, local chemical production rates, rather than by treating

12   different isotopic combinations of nitrate as separate tracers that can be transported in the model. Alexander et al.

13   (2009) transported four nitrate tracers, one each for nitrate production by NO_2+OH, N_2O_5 hydrolysis, NO_3+HC, and

14   nitrate originating from its formation in the stratosphere. Since $\Delta^{17}O(NO_x)$ was not transported in the Alexander et al.

15   (2009) model, it was calculated using local production rates, so effectively only one-third of the $\Delta^{17}O$(nitrate) was

16   transported in Alexander et al. (2009). Accurately accounting for transport of $\Delta^{17}O$(nitrate) in the model would require

17   transporting all individual isotopic combinations of the primary reactant (NO), the final product (nitrate), and each

18   reaction intermediate (e.g., N_2O_5), which we do not do here due to the large computational costs. Thus, the model

19   results shown here represent $\Delta^{17}O$(nitrate) from local NO_x cycling and nitrate production. This may lead to model

20   biases, particularly in remote regions such as polar-regions in winter-time when most nitrate is likely transported from

21   lower latitudes or the stratosphere. This should make little difference in polluted regions where most nitrate is formed

22   locally. This approach will however reflect the full range of possible modeled $\Delta^{17}O$(nitrate) values, which can then

23   be compared to the range of observed $\Delta^{17}O$(nitrate) values.

24

25   The $\Delta^{17}O$(nitrate) value of nitrate produced from each production pathway is calculated as shown in Table 1. The

26   value of A in Table 1 represents the relative importance of the oxidation pathways of NO to NO_2 where the oxygen

27   atom transferred comes from ozone ($NO + O_3$ and $NO + XO$):

Atmospheric
Chemistry
and Physics
Discussions

1     $A = \dfrac{k_{O_3+NO}[O_3]+k_{XO+NO}[XO]}{k_{O_3+NO}[O_3]+k_{XO+NO}[XO]+k_{HO_2+NO}[HO_2]+k_{RO_2+NO}[RO_2]}$ (E1)

2   In E1, k represents the local reaction rate constant for each of the four reactions, XO = BrO, ClO, IO, and OIO, and

3   we assume $\Delta^{17}O(XO)$ is equal to the $\Delta^{17}O$ value of the terminal oxygen atoms of ozone, as described in more detail

4   below. This effectively assumes that the other oxidation pathways (NO + HO$_2$ and NO + RO$_2$) yield $\Delta^{17}O(NO_x) =$

5   0‰. Although HO$_2$ may have a small ^{17}O enrichment on the order of 1-2‰ (Savarino and Thiemens, 1999b), the

6   assumption that this pathway yields $\Delta^{17}O(NO_x) = 0$‰ simplifies the calculation and leads to negligible differences in

7   calculated $\Delta^{17}O(nitrate)$ (Michalski et al., 2003). This approach assumes that NO$_x$ cycling is in photochemical steady-

8   state, which only occurs during the daytime. A is calculated in the model as the 24-hour average NO$_2$ production rate,

9   rather than the daytime average only. As was shown in Alexander et al. (2009), rapid daytime NO$_x$ cycling dominates

10   the calculated 24-hour averaged A value, leading to negligible differences in calculated $\Delta^{17}O(nitrate)$ for 24-hour

11   averaged values versus daytime averaged values.

12

13   NO$_x$ formed during the day will retain its daytime $\Delta^{17}O(NO_x)$ signature throughout the night due to lack of NO$_2$

14   photolysis (Morin et al., 2011), suggesting similar A values for the nighttime reactions (R2, R4, R5, R8, and R10 in

15   Table 1). However, NO emitted at night will retain its originally emitted isotopic signature ($\Delta^{17}O(NO) = 0$‰) due to

16   lack of NO$_x$ cycling under dark conditions. Any NO emitted at night and oxidized to NO$_2$ before sunrise will result

17   in $\Delta^{17}O(NO_2)$ equal to one-half of the $\Delta^{17}O$ value of the oxidant, since only one of the two oxygen atoms of NO$_2$ will

18   originate from the oxidant. Since HO$_x$ abundance is low at night, ozone will be the dominant oxidant. Thus, NO both

19   emitted and oxidized to NO$_2$ at night will lead to $A_{night} = 0.5$ (half of the O atoms of NO$_2$ originate from O$_3$). Since

20   the atmospheric lifetime of NO$_x$ against nighttime oxidation to nitrate (R2+R4+R5) is typically greater than 24 hours

21   (Figure S1), most nitrate formed during the nighttime will form from NO$_x$ that reached photochemical equilibrium

22   during the previous day. Thus, we use values of A calculated as the 24-hour average NO$_2$ production rate for

23   calculating the $\Delta^{17}O(nitrate)$ value of all nitrate production pathways, including those that can occur at night. This is

24   consistent with a box modeling study that explicitly calculated the diurnal variability of $\Delta^{17}O(NO_x)$ and $\Delta^{17}O(nitrate)$

25   suggesting similar (within 5%) values for $\Delta^{17}O(nitrate)$ when assuming the NO$_x$ reached photochemical steady-state

26   versus explicit calculation of diurnal variability of $\Delta^{17}O(NO_x)$ and $\Delta^{17}O(nitrate)$ (Morin et al., 2011). Using 24-hour

27   averaged A values may lead to an overestimate of $\Delta^{17}O(nitrate)$ in locations with more rapid nighttime nitrate

Atmospheric
Chemistry
and Physics
Discussions

1   formation rates such as in China and India (Figure S1). However, even in these locations the lifetime of NO_x against

2   nighttime oxidation is greater than 12 hours, suggesting that over half of nitrate formation at night occurs from the

3   oxidation of NO_x that reached photochemical equilibrium during the daytime. When comparing modeled $\Delta^{17}O$(nitrate)

4   with observations, we add error bars to model values in these locations (Beijing and Mt. Lulin, Taiwan) that reflect

5   the range of possible A values for nighttime nitrate formation, with the high end (A_{high}) reflecting 24-hour average A

6   values and the low end assuming that half of nitrate formation occurs from oxidation of NO_x that reached

7   photochemical equilibrium during the daytime ($A_{low} = 0.5A + 0.5A_{night} = 0.5A + 0.25$).

8

9    $\Delta^{17}O$(nitrate) for total nitrate is calculated in the model according to:

10    $\Delta^{17}O(nitrate) = \sum_{R=R1}^{R10} f_R \Delta^{17}O(nitrate)_R$ (E2)

11   where f_R represents the fractional importance of each nitrate production pathway (R1-R10 in Table 1) relative to total

12   nitrate production, and $\Delta^{17}O$(nitrate)$_R$ is the $\Delta^{17}O$(nitrate) value for each reaction as described in Table 1. To calculate

13    $\Delta^{17}O$(nitrate), we assume that the mean $\Delta^{17}O$ value of the ozone molecule ($\Delta^{17}O(O_3)$) is equal to 26‰ based on recent

14   observations (Vicars et al., 2012;Ishino et al., 2017b;Vicars and Savarino, 2014). Since the ^{17}O enrichment in O_3 is

15   contained entirely in its terminal oxygen atoms (Vicars et al., 2012;Berhanu et al., 2012;Bhattacharya et al.,

16   2008;Savarino et al., 2008;Michalski and Bhattacharya, 2009;Bhattacharya et al., 2014), and it is the terminal oxygen

17   atom that is transferred to the oxidation product during chemical reactions (Savarino et al., 2008;Berhanu et al., 2012),

18   the $\Delta^{17}O$ value of the oxygen atom transferred from ozone to the product is 50% larger than the bulk $\Delta^{17}O(O_3)$ value.

19   Thus, we assume that the $\Delta^{17}O$ value of the oxygen atom transferred from O_3 ($\Delta^{17}O(O_3^*)$) = 1.5 x $\Delta^{17}O(O_3)$ = 39‰, as

20   in previous work (e.g., (Morin et al., 2011)), where $\Delta^{17}O(O_3^*)$ represents the $\Delta^{17}O$ value of the terminal oxygen atoms

21   in ozone.

22

23

24   **3. Results and Discussion**

25

26   Figure 1 shows the relative importance of the different oxidation pathways of NO to NO_2 and nitrate formation below

27   1 km altitude in the model for the "cloud chemistry" simulation, with equivalent values for the "standard" simulation

Atmospheric
Chemistry
and Physics
Open Access
Discussions
EGU

1   shown in parentheses. We focus on model results near the surface because these can be compared to observations;

2   currently only surface observations of $\Delta^{17}O$(nitrate) are available. The dominant oxidant of NO to NO_2 is O_3 (84-

3   85%). Much of the remaining oxidation occurs due to the reaction with peroxy radicals (HO_2 and RO_2). Oxidation of

4   NO to NO_2 by XO is minor (1%) and occurs over the oceans because the main source of tropospheric reactive halogens

5   is from sea salt aerosol and sea water (Chen et al., 2017;Sherwen et al., 2016;Wang et al., 2018) (Figure 2).

6

7   For both the "cloud chemistry" and "standard" simulations, the two most important nitrate formation pathways are

8   NO_2 + OH (41-42%) and N_2O_5 hydrolysis (28-41%) , the latter of which is dominant over the mid- to high-northern

9   continental latitudes during winter where both NO_x emissions and aerosol abundances are relatively large (Figures 1

10   and 3). The "cloud chemistry" simulation results in an equal importance of nitrate formation via NO_2 + OH and N_2O_5

11   hydrolysis (both 41%) due to increases in the rate of N_2O_5 uptake in clouds and decreases in the importance of NO_2

12   hydrolysis, which can compete with N_2O_5 formation at night. In the "standard" model, NO_2 hydrolysis represents an

13   important nitrate production mechanism (12%), but it is negligible in the "cloud chemistry" simulation due to the

14   reduction in the reaction probability (from $\gamma_{NO2} = 10^{-4}$ to $\gamma_{NO2} = 10^{-4}$ to 10^{-8}) in the model, which is supported by

15   laboratory studies (Burkholder et al., 2015;Crowley et al., 2010;Tan et al., 2016). The formation of HNO_3 from the

16   hydrolysis of $RONO_2$ formed from both daytime (NO + RO_2) and nighttime (NO_3 + MTN/ISOP) reactions represents

17   6% of total, global nitrate formation (Figure 1) and is dominant over Amazonia (Figure 3). $RONO_2$ hydrolysis

18   represents up to 20% of inorganic nitrate formation in the southeast U.S. (Figure 3). This is similar to Fisher et al.

19   (2016) who estimated that formation of $RONO_2$ accounts for up to 20% of NO_x loss in this region during summer,

20   with $RONO_2$ hydrolysis representing 60% of $RONO_2$ loss. Globally, the formation of inorganic nitrate from the

21   hydrolysis of $RONO_2$ is dominated by $RONO_2$ formation from the daytime reactions (3-6%), while the formation of

22   $RONO_2$ from nighttime reactions represents up to 3%. The relative importance of nighttime and daytime $RONO_2$

23   formation is expressed as a range because precursors to $RONO_2$ that formed from monoterpenes can form from both

24   daytime and nighttime reactions, and these precursors are not separately diagnosed in the model output. HNO_3

25   formation from NO_3 + HC and the hydrolysis of XNO_3 are small globally (5-6%), but the latter is dominant over the

26   remote oceans (Figure 3).

27

Atmospheric
Chemistry
and Physics
Discussions

1 Figures 4 - 6 show modeled $\Delta^{17}O$(nitrate) for the "cloud chemistry" simulation (the "standard" simulation is shown in

2 Figures S2 – S4). Figure 4 shows modeled annual-mean $\Delta^{17}O$(nitrate) below 1 km altitude. The model predicts an

3 annual-mean range of $\Delta^{17}O$(nitrate) = 4 – 33‰ near the surface. The lowest values are over Amazonia due to the

4 dominance of $RONO_2$ hydrolysis and the highest values are over the mid-latitude oceans due to the dominance of

5 XNO_3 hydrolysis (Figures 3 and 4).

6

7 Figure 5 compares the model with a global compilation of $\Delta^{17}O$(nitrate) observations from around the world.

8 Observations included in Figure 5 include locations where there is enough data to calculate monthly means at each

9 location (McCabe et al., 2006;Kunasek et al., 2008;Hastings et al., 2003;Kaiser et al., 2007;Michalski et al.,

10 2003;Guha et al., 2017;Savarino et al., 2013;Ishino et al., 2017b;Savarino et al., 2007;Alexander et al., 2009;He et al.,

11 2018b). Figure 6 compares the seasonality in modeled $\Delta^{17}O$(nitrate) to the observations where samples were collected

12 over the course of approximately one year (McCabe et al., 2006;Kunasek et al., 2008;Kaiser et al., 2007;Michalski et

13 al., 2003;Guha et al., 2017;Savarino et al., 2013;Ishino et al., 2017b;Savarino et al., 2007;Alexander et al., 2009). In

14 contrast to Alexander et al. (2009), the model does not significantly underestimate the $\Delta^{17}O$(nitrate) observations when

15 assuming $\Delta^{17}O(O_3)$ on the order of 25‰ (see Figure 2d in Alexander et al. (2009)). The increase in modeled

16 $\Delta^{17}O$(nitrate) is due to increased importance of O_3 in NO_x cycling (85% below 1 km) compared to Alexander et al.

17 (2009) (80% below 1 km altitude), and an increase in the number and fractional importance of nitrate formation

18 pathways that yield relatively high values of $\Delta^{17}O$(nitrate) (red pathways in Fig. 1). Although XO species themselves

19 are only a minor NO oxidation pathway (1%), the addition of reactive halogen chemistry in the model has altered the

20 relative abundance of O_3 and HO_x (Sherwen et al., 2016) in such a way as to increase the modeled $\Delta^{17}O(NO_x)$. The

21 Alexander et al. (2009) study used GEOS-Chem v8-01-01, which included tropospheric nitrate formation from the

22 NO + OH, N_2O_5 + H_2O, and NO_3 + HC pathways only. An increased importance of N_2O_5 hydrolysis (R4) and

23 additional nitrate formation pathways that yield relatively high values of $\Delta^{17}O$(nitrate) (R5, R6, R8, and R10) in the

24 present study also explain the increase in modeled $\Delta^{17}O$(nitrate) relative to Alexander et al. (2009). Assuming a value

25 of 35‰ for $\Delta^{17}O(O_3)$ in the model that did not include reactive halogen chemistry or heterogeneous reactions in cloud

26 water produced good agreement between modeled and observed $\Delta^{17}O$(nitrate) in Alexander et al. (2009); however, in

27 the current version of the model this isotopic assumption leads to a model overestimate at nearly all locations (Figure

Atmospheric
Chemistry
and Physics
Discussions

1   S5). The "cloud chemistry" model shows somewhat better agreement with the observations ($R^2 = 0.51$ in Figure 5)

2   compared to the "standard" model ($R^2 = 0.48$ in Figure S3). Improved agreement with the observations occurs in the

3   mid- to high-latitudes (Figures 6 and S4) is due to addition of N_2O_5 hydrolysis in clouds (Figures 3 and S6).

4

5   The mean $\Delta^{17}O(nitrate)$ value of the observations (27.7 ± 5.0‰) shown in Figure 5 is not significantly different from

6   the modeled values at the location of the observations (28.6 ± 4.5‰); however, the range of $\Delta^{17}O(nitrate)$ values of

7   the observations ($10.9 - 40.6$‰) is larger than in the model ($19.6 - 37.6$‰). As previously noted in Savarino et al.

8   (2007), the maximum observed $\Delta^{17}O(nitrate)$ value (40.6‰) is not possible given our isotope assumption for the

9   terminal oxygen atom of ozone ($\Delta^{17}O(O_3^*) = 39$‰). Observed $\Delta^{17}O(nitrate) > 39$‰ (in Antarctica) has been suggested

10   to be due to transport of nitrate from the stratosphere (Savarino et al., 2007), as stratospheric O_3 is expected to have a

11   higher $\Delta^{17}O(O_3)$ value than ozone produced in the troposphere (Krankowsky et al., 2000;Mauersberger et al.,

12   2001;Lyons, 2001). Indeed, the model underestimates the observations at Dumont d'Urville (DDU) and the South

13   Pole (both in Antarctica) during winter and spring (Figure 6), when and where the stratospheric contribution is

14   expected to be most important (Savarino et al., 2007). The model underestimate in Antarctica may also be due to

15   model underestimates of BrO column (Chen et al., 2017) and ozone abundance (Sherwen et al., 2016) in the southern

16   high latitudes. The largest model overestimates occur at Mt. Lulin, Taiwan (Figures 5 and 6). Based on nitrogen

17   isotope observations ($\delta^{15}N$), nitrate at Mt. Lulin is thought to be influenced by anthropogenic nitrate emitted in polluted

18   areas of mainland China and transported to Mt. Lulin, rather than local nitrate production (Guha et al., 2017). The

19   model compares well to the mid-latitude locations close to pollution sources (La Jolla and Princeton), although the

20   model underestimates winter time $\Delta^{17}O(nitrate)$ in La Jolla, CA, USA.

21

22   **4. Model uncertainties**

23   The uncertainty in the two most important nitrate formation pathways, $NO_2 + OH$ and N_2O_5 hydrolysis, and their

24   impacts on NO_x and oxidant budgets, have been examined and discussed elsewhere (Macintyre and Evans,

25   2010;Newsome and Evans, 2017;Holmes et al., 2019). The impacts of the formation and hydrolysis of halogen nitrates

26   on global NO_x and oxidant budgets have also been previously examined (Sherwen et al., 2016). Here we focus on

27   three additional processes using a set of model sensitivity studies. First, we examine the importance of the third most

Atmospheric
Chemistry
and Physics
Discussions

1 important nitrate production pathway on the global scale as predicted by the "standard" model, NO_2 aerosol uptake

2 and hydrolysis, and its implications for the global NO_x, nitrate, and oxidant budgets. Second, we examine the role of

3 changing anthropogenic NO_x emissions over a 15-year period (2000 to 2015) on the relative importance of the

4 formation of inorganic nitrate from the hydrolysis of organic nitrates. Finally, we examine the role of aerosol nitrate

5 photolysis on the relative importance of different nitrate formation pathways. The impact of aerosol nitrate photolysis

6 on NO_x and oxidant budgets has been examined in detail elsewhere (Kasibhatla et al., 2018).

7

8 **4.1 Heterogeneous uptake and hydrolysis of NO_2**

9 Heterogeneous uptake of NO_2 to form HNO_3 and HONO is the third most important nitrate formation pathway in the

10 "standard" model on the global scale (Figure 1). The reaction probability (γ_{NO2}) measured in laboratory studies ranges

11 between 10^{-8} to 10^{-4} depending on aerosol chemical composition (Lee and Tang, 1988;Crowley et al., 2010;Gutzwiller

12 et al., 2002;Yabushita et al., 2009;Abbatt and Waschewsky, 1998;Burkhart et al., 2015;Broske et al., 2003;Li et al.,

13 2018a;Xu et al., 2018). A value of $\gamma_{NO2} = 10^{-4}$ is used in the "standard" model, which is at the high end of the reported

14 range. A molar yield of 0.5 for both HNO_3 and HONO formation is assumed in the model based on laboratory studies

15 and hypothesized reaction mechanisms (Finlayson-Pitts et al., 2003;Jenkin et al., 1988;Ramazan et al., 2004;Yabushita

16 et al., 2009). However, both the reaction rate and mechanism of this reaction and its dependence on chemical

17 composition and pH is still not well understood (Spataro and Ianniello, 2014).

18

19 The "cloud chemistry" simulation uses a reaction probability formulation for aerosol uptake of NO_2 (γ_{NO2}) that

20 depends on aerosol chemical composition, ranging from $\gamma_{NO2} = 10^{-8}$ for dust to $\gamma_{NO2} = 10^{-4}$ for black carbon based on

21 recent laboratory studies (Holmes et al., 2019). The updated NO_2 reaction probability results in a negligible (<1%)

22 importance of this reaction for nitrate formation, compared to 12% contribution in the "standard" model. The "cloud

23 chemistry" simulation significantly increases the fractional importance of N_2O_5 hydrolysis (from 28 to 41%, globally

24 below 1 km altitude) compared to the "standard" simulation, in part due to decreased competition from NO_2 hydrolysis

25 and in part due to increased N_2O_5 hydrolysis in clouds. To evaluate the relative importance of competition from NO_2

26 hydrolysis and the addition of N_2O_5 hydrolysis in clouds, we perform a model sensitivity study that is the same as the

27 "standard" simulation but decreases the reaction probability of NO_2 hydrolysis on aerosol ($\gamma_{NO2} = 10^{-7}$), without adding

28 N_2O_5 hydrolysis in clouds. Similar to the "cloud chemistry" simulation, using $\gamma_{NO2} = 10^{-7}$ renders NO_2 hydrolysis a

1   negligible nitrate formation pathway, and increases the relative importance of N_2O_5 hydrolysis from 28% to 37%.

2   This suggests that reduced competition from NO_2 hydrolysis is the main reason for the increased importance of N_2O_5

3   hydrolysis in the "cloud chemistry" simulation, though the addition of heterogeneous reactions on clouds also plays a

4   role.

5

6   NO_2 hydrolysis represents a significant source of HONO in the "standard" model simulation; the reduced NO_2 reaction

7   probability from $\gamma_{NO2} = 10^{-4}$ to $\gamma_{NO2} = 10^{-7}$ results in a reduction of HONO below 1 km altitude by up to 100% over

8   the continents, with relatively small (up to 1 ppb) changes in nitrate concentrations (Figure 7). The reduction in the

9   rate of heterogeneous NO_2 uptake leads to reductions in OH where this reaction was most important in the model

10   (over China and Europe) due to reductions in HONO, but leads to increases in OH elsewhere due to increases in ozone

11   (by up to a few ppb) resulting from small increases in the NO_x lifetime due to a reduction in the NO_x sink (Figure 8).

12   Similar changes in HONO are seen when comparing the "standard" and "cloud chemistry" simulation (not shown).

13   Increased importance of N_2O_5 hydrolysis in both the "cloud chemistry" simulation and the simulation without cloud

14   chemistry but with a reduced reaction probability for NO_2 hydrolysis increases modeled annual-mean $\Delta^{17}O$(nitrate)

15   by up to 3‰ in China where this reaction is most important. This improves model agreement with monthly-mean

16   observations of $\Delta^{17}O$(nitrate) in Beijing (He et al., 2018a) (Figures 5 and S3).

17

18   The product yields of NO_2 hydrolysis are also uncertain. Jenkin et al. (1988) proposed the formation of a water

19   complex, $NO_2 \cdot H_2O$, leading to the production of HONO and HNO_3. Finlayson-Pitts et al. (2003) and Ramazan et al.

20   (2004) proposed the formation of the dimer N_2O_4 on the surface, followed by isomerization to form $NO^+NO_3^-$.

21   Reaction of $NO^+NO_3^-$ with H_2O results in the formation of HONO and HNO_3. Laboratory experiments by Yabushita

22   et al. (2009) suggested that dissolved anions catalyzed the dissolution of NO_2 to form a radical intermediate $X-NO_2^-$

23   (where X = Cl, Br, or I) at the surface followed by reaction with $NO_2(g)$ to form HONO and NO_3^-. These experiments

24   described above were performed at NO_2 concentrations much higher than exist in the atmosphere (10 – 100 ppm)

25   (Yabushita et al., 2009;Finlayson-Pitts et al., 2003;Ramazan et al., 2004). A laboratory study utilizing isotopically

26   labeled water to investigate the reaction mechanism suggested that the formation of HONO resulted from the reaction

27   between adsorbed NO_2 and H^+, while the formation of HNO_3 resulted from the reaction between adsorbed NO_2 and

28   OH^-, and did not involve the N_2O_4 intermediate (Gustafsson et al., 2009). Results from Gustafsson et al. (2009)

Atmospheric
Chemistry
and Physics
Discussions

1   suggest an acidity-dependent yield of HONO and HNO_3, favoring HONO at low pH values. A recent study in the

2   northeast U.S. during winter found that modeled nitrate abundance was overestimated using a molar yield of 0.5 for

3   HONO and HNO_3, and the model better matched the observations of NO_2 and nitrate when assuming a molar yield of

4   1.0 for HONO (Jaeglé et al., 2018). Particles were acidic (pH < 2) during this measurement campaign (Guo et al.,

5   2017;Shah et al., 2018), which may favor HONO production over HNO_3.

6

7   We examine the potential importance of this acidity-dependent yield by implementing a pH-dependent product yield

8   in two separate sensitivity simulations, first using an NO_2 aerosol uptake reaction probability of $\gamma = 10^{-4}$ as in the

9   "standard" simulation and second with $\gamma_{NO2} = 10^{-7}$. The acidity-dependent yield for HONO and HNO_3 formation is

10   based on the laboratory study by Gustafsson et al. (2009). We use aerosol pH calculated from ISORROPIA II

11   (Fountoukis and Nenes, 2007) to calculate the concentration of $[H^+]$ and $[OH^-]$ in aerosol water. The yield of HONO

12   (Υ_{HONO}) from heterogeneous uptake of NO_2 on aerosol surfaces is calculated according to E3:

13   $\Upsilon_{HONO} = \frac{[H^+]}{[H^+]+[OH^-]}$ (E3)

14   where $[H^+]$ and $[OH^-]$ are in units of M. The yield of HNO_3 from this reaction is equal to (1 - Υ_{HONO}). E3 yields values

15   of Υ_{HONO} near unity for aerosol pH values less than 6, decreasing rapidly to zero between pH values between 6-8

16   (Figure 9). Calculated aerosol pH values are typically < 6 in the model except in remote regions far from NO_x sources

17   (Figure S7), favoring the product HONO.

18

19   The acidity-dependent yield implemented in the "standard" simulation with $\gamma_{NO2} = 10^{-4}$ increases HONO

20   concentrations by up to 1 ppbv in China where this reaction is most important (Figure 10). Fractional increases in

21   HONO exceed 100% in remote locations (Figure 10).   Increased HONO leads to increases in OH on the order of 10

22   – 20% in most locations below 1 km altitude, while ozone concentrations increase in most locations by up to several

23   ppbv (Figure 10). The exception is the southern high latitudes; likely due to decreased formation and thus transport

24   of nitrate to remote locations. The impact on NO_x and nitrate budgets is relatively minor. The global, annual mean

25   NO_x burden near the surface (below 1 km) increases slightly (+2%) as a result of the decreased rate of conversion of

26   NO_2 to nitrate; the change to the global tropospheric burden is negligible. Annual-mean surface nitrate concentrations

27   show small decreases up to 1 ppbv in China where this reaction is most important in the model; impacts on nitrate

28   concentrations over a shorter time period may be more significant (Jaeglé et al., 2018). The fraction of HNO_3 formed

Atmospheric
Chemistry
and Physics
Discussions

1   from NO_2 + OH (49%) increases due to increases in OH from the HONO source. The fraction of HNO_3 formation

2   from the uptake and hydrolysis of N_2O_5 also increases (from 28% to 32%) due to reductions in the nighttime source

3   of nitrate from NO_2 hydrolysis. The calculated mean $\Delta^{17}O$(nitrate) at the location of the observations shown in Figure

4   5 (27.9 ± 5.0‰) is not significantly impacted due to compensating effects from changes in both high- and low-

5   producing $\Delta^{17}O$(nitrate) values. Modeled monthly mean $\Delta^{17}O$(nitrate) in China, where NO_2 hydrolysis is most

6   important increases by ~1‰, but is still biased low by 1-2‰.

7

8   Using a combination of both the low reaction probability ($\gamma = 10^{-7}$) and the acidity-dependent yield gives similar results

9   as using $\gamma = 10^{-7}$ and assuming a molar yield of 0.5 for HONO and HNO_3 (not shown). In other words, including a

10   pH-dependent product yield rather than a yield of 0.5 for HONO and nitrate results in negligible differences for

11   oxidants, NO_x and nitrate abundances when the reaction probability (γ_{NO2}) is low.

12

13   **4.2 Hydrolysis of organic nitrates ($RONO_2$)**

14   Anthropogenic NO_x emissions have been increasing in China and decreasing in the U.S. and Europe (Richter et al.,

15   2005;Hoesly et al., 2018b), with implications for the relative importance of inorganic and organic nitrate formation as

16   a sink for NO_x (Zare et al., 2018). To examine the impacts of recent changes in anthropogenic NO_x emissions for

17   nitrate formation pathways, we run the "standard" model using the year 2000 emissions and meteorology after a 1-

18   year model spin up, and compare the results to the "standard" model simulation run in the year 2015. This time-period

19   encompasses significant changes in anthropogenic NO_x emissions in the U.S., Europe, and China, and encompasses

20   most of the time period of the observations shown in Figures 5 and 6. Total, global anthropogenic emissions of NO_x

21   are slightly lower in the 2000-year simulation (30 Tg N yr^{-1}) compared to the year 2015 simulation (31 Tg N yr^{-1}) due

22   to decreases in North America and Europe, counteracted by increases in Asia (Figure S7). This leads to increases of

23   less than 10% in the annual-mean, fractional importance of the source of nitrate from the hydrolysis of organic nitrates

24   in the U.S., and corresponding decreases of less than 10% over China (Figure 11). Relatively small changes (< 10%)

25   in nitrate formation pathways yield small changes (< 2‰) in modeled annual-mean $\Delta^{17}O$(nitrate) between the year

26   2000 and 2015, differences in $\Delta^{17}O$(nitrate) over shorter time periods may be larger. Changes in the formation of

27   nitrate from the hydrolysis of $RONO_2$ remains unchanged globally, as increases in the U.S. and Europe and decreases

28   in China counteract one another.

4.3 Photolysis of aerosol nitrate

Observations have demonstrated that aerosol nitrate can be photolyzed at rates much faster than $HNO_3(g)$ (Reed et al., 2017;Ye et al., 2016); however, the magnitude of the photolytic rate constant is uncertain. We examine the implications of this process for global nitrate formation pathways by implementing the photolysis of aerosol nitrate as described in Kasibhatla et al. (2018) into the "standard" model simulation, scaling the photolytic rate constant for both fine- and coarse-mode aerosol nitrate to a factor of 25 times higher than that for $HNO_3(g)$ (Kasibhatla et al., 2018;Romer et al., 2018), with a molar yield of 0.67 for HONO and 0.33 for NO_x production. The global, annual mean NO_x burden near the surface (below 1 km) increases slightly (+2%) as a result of the photolytic recycling of nitrate to NO_x, similar to Kasibhatla et al. (2018). Aerosol nitrate photolysis results in only small impacts on the relative importance of nitrate formation pathways (< 2%) likely due to simultaneous increases in O_3 and OH (Kasibhatla et al., 2018), which in turn yields small impacts on calculated $\Delta^{17}O(nitrate)$ at the location of the observations shown in Figure 5 (27.9 ± 5.0‰). Nitrate photolysis itself has minimal impact on $\Delta^{17}O(nitrate)$ because it is a mass-dependent process (McCabe et al., 2005).

5   Conclusions

Observations of $\Delta^{17}O(nitrate)$ can be used to help quantify the relative importance of different nitrate formation pathways. Interpretation of $\Delta^{17}O(nitrate)$ requires knowledge of $\Delta^{17}O(O_3)$, which until recently was highly uncertain. Previous modeling studies showed good agreement between observed and modeled $\Delta^{17}O(nitrate)$ when assuming $\Delta^{17}O(O_3)$ = 35‰. However, recent observations of $\Delta^{17}O(O_3)$ from around the world have shown $\Delta^{17}O(O_3)$ = 26 ± 1‰, suggesting that models are underestimating the role of ozone relative to HO_x in NO_x chemistry. We utilize a global compilation of observations of $\Delta^{17}O(nitrate)$ to assess the representation of nitrate formation in a global chemical transport model (GEOS-Chem). The modeled $\Delta^{17}O(nitrate)$ is roughly consistent with observations, with a mean modeled and observed $\Delta^{17}O(nitrate)$ of (28.6 ± 4.5‰) and (27.6 ± 5.0‰), respectively, at the locations of the observations. Improved agreement between modeled and observed $\Delta^{17}O(nitrate)$ is due to increased importance of ozone versus HO_2 and RO_2 in NO_x cycling and an increase in the number and importance of nitrate production pathways that yield high $\Delta^{17}O(nitrate)$ values. The former may be due to implementation of tropospheric reactive

1   halogen chemistry in the model, which impacts ozone and HO_x abundances. The latter is due mainly to increases in

2   the relative importance of N_2O_5 hydrolysis, with the hydrolysis of halogen nitrates also playing an important role in

3   remote regions.

4

5   The main nitrate formation pathways in the model below 1 km altitude are from $NO_2 + OH$ and N_2O_5 hydrolysis (both

6   41%). The relative importance of global nitrate formation from the hydrolysis of halogen nitrates and hydrogen-

7   abstraction reactions involving the nitrate radical (NO_3) are of similar magnitude (~5%). The formation of nitrate

8   from the hydrolysis of organic nitrate has increased slightly in the U.S. and decreased in China (changes <10%) due

9   to changing NO_x emissions from the year 2000 to 2015, although the global mean fractional importance (6%) remains

10   unchanged as the regional changes counteract one another. Nitrate formation via heterogeneous NO_2 and NO_3 uptake

11   and $NO_2 + HO_2$ are negligible (<2%). Although aerosol nitrate photolysis has important implications for O_3 and OH,

12   the impacts on nitrate formation pathways are small.

13

14   The model parameterization for heterogeneous uptake of NO_2 has significant impacts on HONO and oxidants (OH

15   and ozone) in the model. HONO production from this reaction has been suggested to be an important source of OH

16   in Chinese haze due to high NO_x and aerosol abundances (Hendrick et al., 2014;Tong et al., 2016;Wang et al., 2017),

17   with implications for the gas-phase formation of sulfate aerosol from the oxidation of sulfur dioxide by OH (Shao et

18   al., 2018;Li et al., 2018b). More recent laboratory studies suggest that the reaction probability of NO_2 on aerosols is

19   lower than that previously used in the model. Using an NO_2 reaction probability formulation that depends on the

20   chemical composition of aerosols as described in Holmes et al. (2019) renders this reaction negligible for nitrate

21   formation, and has significant implications for modeled HONO, ozone, and OH. Although uncertainty also exists in

22   the relative yield of nitrate and HONO from this reaction, the impacts of this assumption are negligible when we use

23   these updated NO_2 reaction probabilities. Observations of $\Delta^{17}O$(nitrate) in Chinese haze events during winter (He et

24   al., 2018b) may help to quantify the importance of this nitrate production pathway in a region where the model predicts

25   it is significant.

26

27   Author contributions: B.A. designed the study and performed the model simulations and calculations. All other

28   authors provided model code and contributed to writing and analysis.

1

6

7   **References**

8   Abbatt, J. P. D., and Waschewsky, G. C. G.: Heterogeneous interactions of OHBr, HNO_3, O_3, and NO_2 with
9   deliquescent NaCl aerosols at room temperature, J. Phys. Chem. A, 102, 3719-3725, 1998.

10   Alexander, B., Savarino, J., Kreutz, K. J., and Thiemens, M. H.: Impact of preindustrial biomass-burning emissions
11   on the oxidation pathways of tropospheric sulfur and nitrogen, J. Geophys. Res., 109, D08303, doi:
12   10.1029/2003JD004218, 2004.

13   Alexander, B., Hastings, M. G., Allman, D. J., Dachs, J., Thornton, J. A., and Kunasek, S. A.: Quantifying
14   atmospheric nitrate formation pathways based on a global model of the oxygen isotopic composition ($D^{17}O$) of
15   atmospheric nitrate, Atmos. Chem. Phys., 9, 5043-5056, 10.5194/acp-9-5043-2009, 2009.

16   Berhanu, T. A., Savarino, J., Bhattacharya, S. K., and Vicars, W. C.: ^{17}O excess transfer during the $NO_2 + O_3 \rightarrow$
17   $NO_3 + O_2$ reaction, J. Chem. Phys., 136, 044311, doi: 10.1063/1.3666852, 2012.

18   Bertram, T. H., and Thornton, J. A.: Toward a general parameterization of N2O5 reactivity on aqueous particles: the
19   competing effects of particle liquid water, nitrate and chloride, Atmos. Chem. Phys, 9, 8351-8363, 10.5194/acp-9-
20   8351-2009, 2009.

21   Bey, I., Jacob, D. J., Yantosca, R. M., Logan, J. A., Field, B. D., Fiore, A. M., Li, Q., Liu, H. Y., Mickley, L. J., and
22   Schultz, M. G.: Global modeling of tropospheric chemistry with assimilated meteorology: Model description and
23   evaluation, J. Geophys. Res., 106, 23073-23095, 2001.

24   Bhattacharya, S. K., Pandey, A., and Savarino, J.: Determination of intramolecular isotope distribution of ozone by
25   oxidation reaction with silver metal, J. Geophys. Res, 113, D03303, doi:10.1029/2006JF008309, 2008.

26   Bhattacharya, S. K., Savarino, J., Michalski, G., and Liang, M.-C.: A new feature in the internal heavy isotope
27   distribution in ozone, J. Chem. Phys., 141, 10.1063/1.4895614, 2014.

28   Broske, R., Kleffmann, J., and Wiesen, P.: Heterogeneous conversion of NO2 on secondary organic aerosol
29   surfaces: A possible source of nitrous acid (HONO) in the atmosphere?, Atmos. Chem. Phys, 3, 469-474,
30   10.5194/acp-3-469-2003, 2003.

31   Brothers, L. A., Dominguez, G., Fabian, P., and Thiemens, M. H.: Using multi-isotope tracer methods to understand
32   the sources of nitrate in aerosols, fog and river water in Podocarpus National Forest, Ecuador, Eos Trans. AGU, 89,
33   Abstract A11C-0136, 2008.

34   Browne, E. C., and Cohen, R. C.: Effects of biogenic nitrate chemistry on the NOx lifetime in remost continental
35   regions, Atmos. Chem. Phys, 12, 11917-11932, 10.5194/acp-12-11917-2012, 2014.

Atmospheric
Chemistry
and Physics
Discussions

Burkhart, J. F., Sander, S. P., Abbatt, J. P. D., Barker, J. R., Huie, R. E., Kolb, C. E., Kurylo, M. J., Orkin, V. L., Wilmouth, D. M., and Wine, P. H.: Chemical Kinetics and Photochemical Data for Use in Atmospheric Studies, Jet Propulsion Laboratory, Pasadena, CA, USA, 2015.

Burkholder, J. B., Sander, S. P., Abbatt, J. P. D., Barker, J. R., Huie, R. E., Kolb, C. E., Kurylo, M. J., Orkin, V. L., Wilmouth, D. M., and Wine, P. H.: Chemical kinetics and photochemical data for use in atmospheric studies: evaluation number 18, Jet Propulsion Laboratory, Pasadena, CA, 2015.

Chen, Q., Schmidt, J. A., Shah, V., Jaeglé, L., Sherwen, T., and Alexander, B.: Sulfate production by reactive bromine: Implications for the global sulfur and reactive bromine budgets, Geophys. Res. Lett., 44, 7069-7078, 10.1002/2017GL073812, 2017.

Chen, Q., Edebeli, J., McNamara, S. M., Kulju, K., May, N. W., Bertman, S. P., Thanekar, S., Fuentes, J. D., and Pratt, K. A.: HONO, Particulate Nitrite, and Snow Nitrite at a Midlatitude Urban Site during Wintertime, ACS Earth Space Chem., 10.1021/acsearthspacechem.9b00023, 2019.

Costa, A. W., Michalski, G., Schauer, A. J., Alexander, B., Steig, E. J., and Shepson, P. B.: Analysis of atmospheric inputs of nitrate to a temperate forest ecosystem from $D^{17}O$ isotope ratio measurements, Geophys. Res. Lett., 38, L15805, doi:10.1029/2011GL047539, 2011.

Crowley, J. N., Ammann, M., Cox, R. A., Hynes, R. G., Jenkin, M. E., Mellouki, A., Rossi, M. J., Troe, J., and Wallington, T. J.: Evaluated kinetic and photochemical data for atmospheric chemistry: Volume V – heterogeneous reactions on solid substrates, Atmos. Chem. Phys, 10, 9059-9223, 10.5194/acp-10-9059-2010, 2010.

Domine, F., and Shepson, P. B.: Air-Snow Interactions and Atmospheric Chemistry, Science, 297, 1506, 2002.

Dubey, M. K., Mohrschladt, R., Donahue, N. M., and Anderson, J. G.: Isotope-specific kinetics of hydroxyl radical (OH) with water (H_2O): Testing models of reactivity and atmospheric fractionation, J. Phys. Chem. A, 101, 1494-1500, 1997.

Evans, M. J., and Jacob, D. J.: Impact of new laboratory studies of N_2O_5 hydrolysis on global model budgets of tropospheric nitrogen oxides, ozone, and OH, Geophys. Res. Lett., 32, L09813, doi:10.1029/2005GL022469, 2005.

Ewing, S. A., Michalski, G., Thiemens, M., Quinn, R. C., Macalady, J. L., Kohl, S., Wankel, S. D., Kendall, C., McKay, C. P., and Amundson, R.: Rainfall limit of the N cycle on Earth, Global Biogeochemical Cycles, 21, GB3009, 10.1029/2006gb002838, 2007.

Finlayson-Pitts, B. J., Wingen, L. M., Sumner, A. L., Syomin, D., and Ramazan, K. A.: The heterogeneous hydrolysis of NO_2 in laboratory systems and in outdoor and indoor atmospheres: An integrated mechanism, Phys. Chem. Chem. Phys., 5, 223-242, 2003.

Fisher, J. A., Jacob, D. J., Travis, K. R., Kim, P. S., Marais, E. A., Miller, C. C., Yu, K., Zhu, L., Yantosca, R. M., Sulprizio, M. P., Mao, J., Wennberg, P. O., Crounse, J. D., Teng, A. P., Nguyen, T. B., St. Clair, J. M., Cohen, R. C., Romer, P., Nault, B. A., Wooldridge, P. J., Jimenez, J. L., Campuzano-Jost, P., D.A., D., Hu, W., Shepson, P. B., Wiong, F., Blake, D. R., Goldstein, A. H., Misztal, P. K., Hanisco, T. F., Wolfe, G. M., Ryerson, T. B., Wisthaler, A., and Mikoviny, T.: Organic nitrate chemistry and its implications for niteogen budgets in an isoprene- and mooterpene-rich atmosphere: constraints from aircraft (SEAC^{4}RS) and ground-based (SOAS) observations in the Southeast US, Atmos. Chem. Phys, 16, 5969-5991, 10.5194/acp-16-5969-2016, 2016.

Fisher, J. A., Atlas, E. L., Barletta, B., Meinardi, S., Blake, D. R., Thompson, C. R., Ryerson, T. B., Peischl, J., Tzompa-Sosa, Z. A., and Murray, L. T.: Methyl, Ethyl, and Propyl Nitrates: Global Distribution and Impacts on Reactive Nitrogen in Remote Marine Environments, J. Geophys. Res., 123, 12,429-412,451, doi.org/10.1029/2018JD029046, 2018.

Fountoukis, C., and Nenes, A.: ISORROPIA II: a computationally efficient thermodynamic equilibrium model for K^+-Ca^{2+}-Mg^{2+}-NH_4^+-Na^+-SO_4^{2-}-NO_3^--Cl^--H_2O aerosols, Atmos. Chem. Phys., 7, 4639-4659, 2007.

Geng, L., Cole-Dai, J., Alexander, B., Savarino, J., Schauer, A. J., Steig, E. J., Lin, P., and Zatko, M. C.: On the origin of the occasional springtime nitrate concentration maximum in Greenland snow, Atmos. Chem. Phys. Discuss., 14, 9401-9437, 10.5194/acpd-14-9401-2014, 2014.

Geng, L., Murray, L. T., Mickley, L. J., Lin, P., Fu, Q., Schauer, A. J., and Alexander, B.: Isotopic evidence of multiple controls on atmospheric oxidants over climate transitions, Nature, 546, 133-136, 10.1038/nature22340, 2017.

Guha, T., Lin, C. T., Bhattacharya, S. K., Mahajan, A. S., Ou-Yang, C.-F., Lan, Y.-P., Hsu, S. C., and Liang, M.-C.: Isotopic ratios of nitrate in aerosol samples from Mt. Lulin, a high-altitude station in Central Taiwan, Atmos. Env., 154, 53-69, 10.1016/j.atmosenv.2017.01.036, 2017.

Guo, H., Weber, R. J., and Nenes, A.: High levels of ammonia do not raise fine particle pH sufficiently to yield nitrogen oxide-dominated sulfate production, Scientific Reports, 7, 1-7, 10.1038/s41598-017-11704-0, 2017.

Gustafsson, R. J., Kyiakou, G., and Lambert, R. M.: The molecular methanism of tropospheric nitrous acid production on mineral dust surfaces, Chem. Phys. Chem., 9, 1390-1393, 10.1002/cphc.200800259, 2009.

Gutzwiller, L., George, C., Rossler, E., and Ammann, J.: Reaction Kinetics of NO_2 with Resorcinol and 2,7-Naphthalenediol in the Aqueous Phase at Different pH, J. Phys. Chem. A, 106, 12045-12050, 10.1021/jp026240d, 2002.

Hastings, M. G., Sigman, D. M., and Lipschultz, F.: Isotopic evidence for source changes of nitrate in rain at Bermuda, J. Geophys. Res., 108, 4790, doi:10.1029/2003JD003789, 2003.

He, P., Alexander, B., Geng, L., Chi, X., Fan, S., Zhan, H., Kang, H., Zheng, G., Cheng, Y., Su, H., Liu, C., and Xie, Z.: Isotopic constraints on heterogeneous sulfate production in Beijing haze, Atmos. Chem. Phys, 18, 5515-5528, 10.5194/acp-18-5515-2018 2018a.

He, P., Xie, Z., Chi, X., Yu, X., Fan, S., Kang, H., Liu, C., and Zhan, H.: Atmospheric $D^{17}O(NO_3^-)$ reveals nocturnal chemistry dominates nitrate production in Beijing haze, Atmos. Chem. Phys, 18, 14465–14476, 10.5194/acp-18-14465-2018, 2018b.

Hendrick, F., Muller, J.-F., Clemer, K., Wang, P., De Maziere, M., Fayt, C., Gielen, C., Hermans, C., Ma, J. Z., Pinardi, G., Stavrakou, T., Vlemmix, T., and Van Roosendael, M.: Four years of ground-based MAX-DOAS observations of HONO and NO_2 in the Beijing area, Atmos. Chem. Phys, 14, 765-781, 10.5194/acp-14-765-2014, 2014.

Hoesly, R. M., Smith, S. J., Feng, L., Klimont, Z., Janssens-Maenhout, G., Pitkanen, T., Seibert, J. J., Vu, L., Andres, R. J., Bolt, R. M., Bond, T. C., Dawidowski, L., Kholod, N., Kurokawa, J.-I., Li, M., Liu, L., Lu, Z., Moura, M. C. P., O'Rourke, P. R., and Zhang, Q.: Historical (17502014) anthropogenic emissions of reactive gases and aerosols from the Community Emissions Data System (CEDS), Geosci. Model Dev., 11, 369-408, 10.5194/gmd-11-369-2018, 2018a.

Hoesly, R. M., Smith, S. J., Feng, L., Klimont, Z., Janssens-Maenhout, G., Pitkanen, T., Seibert, J. J., Vu, L., Andres, R. J., Bolt, R. M., Bond, T. C., Dawidowski, L., Kholod, N., Kurokawa, J., Li, M., Liu, L., Lu, Z., Moura, M. C. P., O'Rourke, P. R., and Zhang, Q.: Historical (1750–2014) anthropogenic emissions of reactive gases and aerosols from the Community Emissions Data System (CEDS), Geosci. Model Dev., 11, 369-408, 10.5194/gmd-11-369-2018, 2018b.

1 Holmes, C. D., Prather, M. J., and Vinken, G. C. M.: The climate impact of ship NOx emissions: an improved
2 estimate accounting for plume chemistry, Atmos. Chem. Phys, 14, 6801-6812, 10.5194/acp-14-6801-2014, 2014.

3 Holmes, C. D., Bertram, T. H., Confer, K. L., Graham, K. A., Ronan, A. C., Wirks, C. K., and Shah, V.: The role of
4 clouds in the tropospheric NOx cycle: a new modeling approach for cloud chemistry and its global implications,
5 Geophys. Res. Lett., 10.1029/2019GL081990, 2019.

6 Horowitz, L. W., Fiore, A. M., Milly, G. P., Cohen, R. C., Perring, A., Wooldridge, P. J., Hess, P. G., Emmons, L.
7 K., and Lamarque, J.-F.: Observational constraints on the chemistry of isoprene nitrates over the eastern United
8 States, J. Geophys. Res, 112, D12S08, doi:10.1029/2006JD007747, 2007.

9   Hudman, R. C., Moore, N. E., Martin, R. V., Russell, A. R., Mebust, A. K., Valin, L. C., and Cohen, R. C.: A
10 mechanistic model of global soil nitric oxide emissions: implementation and space based-constraints, Atmos. Chem.
11 Phys, 12, 7779-7795, 10.5194/acp-12-7779-2012, 2012.

12 Ishino, S., Hattori, S., Savarino, J., Jourdain, B., Preunkert, S., Legrand, M., Caillon, N., Barbero, A., Kuribayashi,
13 K., and Yoshida, N.: Seasonal variations of triple oxygen isotopic compositions of atmospheric sulfate, nitrate, and
14 ozone at Dumont d'Urville, coastal Antarctica, Atmos. Chem. Phys, 17, 3713-3727, 10.5194/acp-17-3713-2017,
15 2017a.

16 Ishino, S., Hattori, S., Savarino, J., Jourdain, B., Preunkert, S., Legrand, M., Caillon, N., Barbero, A., Kurlbayashi,
17 K., and Yoshida, N.: Seasonal variations of triple oxygen isotopic compositions of atmospheric sulfate, nitrate, and
18 ozone at Dumont d'Urville, coastal Antarctica, Atmos. Chem. Phys, 17, 3713-3727, 10.5194/acp-17-3713-2017,
19 2017b.

20 Jacob, D. J.: Heterogeneous chemistry and tropospheric ozone, Atmos. Env., 34, 2131-2159, 2000.

21 Jacobs, M. I., Burke, W. J., and Elrod, M. J.: Kinetics of the reactions of isoprene-derived hydroxynitrates: gas
22 phase epoxide formation and solution phase hydrolysis,, Atmos. Chem. Phys, 2014, 8933–8946, 10.5194/acp-14-
23 8933-2014, 2014.

24 Jaeglé, L., Steinberger, L., Martin, R. V., and Chance, K.: Global partitioning of NO_x sources using satellite
25 observations: Relative roles of fossil fuel combustion, biomass burning and soil emissions, Faraday Discussions,
26 130, 407-423, DOI: 10.1039/b502128f, 2005.

27 Jaeglé, L., Shah, V., Thornton, J. A., Lopez-Hilfiker, F. D., Lee, B. H., McDuffie, E. E., Fibiger, D., Brown, S. S.,
28 Veres, P., Sparks, T. L., Ebben, C. J., Wooldridge, P. J., Kenagy, H. S., Cohen, R. C., Weinheimer, A. J., Campos,
29 T. L., Montzka, D. D., Digangi, J. P., Wolfe, G. M., Hanisco, T., Schroder, J. C., Campuzano-Jost, P., Day, D. A.,
30 Jimenez, J. L., Sullivan, A. P., Guo, H., and Weber, R. J.: Nitrogen oxides emissions, chemistry, deposition, and
31 export over the Northeast United States during the WINTER aircraft campaign, J. Geophys. Res., 123, 12,368–
32 312,393, doi.org/10.1029/2018JD029133, 2018.

33 Jenkin, M. E., Cox, R. A., and Williams, D. J.: Laboratory studies of the kinetics of formation of nitrous acid from
34 the thermal reaction of nitrogen dioxide and water vapor, Atm. Env., 22, 487-498, 1988.

35 Johnston, J. C., and Thiemens, M. H.: The isotopic composition of tropospheric ozone in three environments, J.
36 Geophys. Res., 102, 25395-25404, 1997.

37 Kaiser, J., Hastings, M. G., Houlton, B. Z., Rockmann, T., and Sigman, D. M.: Triple Oxygen Isotope Analysis of
38 Nitrate Using the Denitrifier Method and Thermal Decomposition of N_2O, Anal. Chem., 79, 599-607, 2007.

39 Kasibhatla, P., Sherwen, T., Evans, M. J., Carpenter, L. J., Reed, C., Alexander, B., Chen, Q., Sulprizio, M. P., Lee,
40 J. D., Read, K. A., Bloss, W. J., Crilley, L. R., Keene, W. C., Pzenny, A. A. P., and Hodzic, H.: Global impact of

Atmospheric
Chemistry
and Physics
Discussions

1 nitrate photolysis of sea-salt aerosol on NOx, OH and ozone in the marine boundary layer, Atmos. Chem. Phys, 18,
2 11185-11203, 10.5194/acp-18-11185-2018 2018.

3 Krankowsky, D., Bartecki, F., Klees, G. G., Mauersberger, K., Schellenback, K., and Stehr, J.: Measurement of
4 heavy isotope enrichment in tropospheric ozone, Geophys. Res. Lett., 22, 1713-1716, 1995.

5 Krankowsky, D., Lammerzahl, P., and Mauersberger, K.: Isotopic measurements of stratospheric ozone, Geophys.
6 Res. Lett., 27, 2593-2595, 2000.

7 Kunasek, S. A., Alexander, B., Hastings, M. G., Steig, E. J., Gleason, D. J., and Jarvis, J. C.: Measurements and
8 modeling of D^{17}O of nitrate in a snowpit from Summit, Greenland, J. Geophys. Res. , 113, D24302,
9 10.1029/2008JD010103, 2008.

10 Lee, C., Martin, R. V., van Donkelaar, A., Lee, H., Dickerson, R. R., Hains, J. C., Krotkov, N., Richter, A., innikov,
11 K., and Schwab, J. J.: SO$_2$ emissions and lifetimes: Estimates from inverse modeling using in situ and global, space-
12 based (SCIAMACHY and OMI) observations, J. Geophys. Res., 116, D06304, 10.1029/2010JD014758, 2011.

13 Lee, J. H., and Tang, I. N.: Accommodation coefficient of gaseous NO$_2$ on water surfaces, Atm. Env., 22, 1988.

14 Li, L., Duan, Z., Li, H., Zhu, C., Henkelman, G., Francisco, J. S., and Zeng, X. C.: Formation of HONO from the
15 NH3-promoted hydrolysis

16 of NO2 dimers in the atmosphere, Proc. Natl. Acad. Sci., 115, 7236–7241, 10.1073/pnas.1807719115, 2018a.

17 Li, L., Hoffmann, M. R., and Colussi, A. J.: Role of Nitrogen Dioxide in the Production of Sulfate during Chinese
18 Haze-Aerosol Episodes, Env. Sci. & Tech., 52, 2686-2693, 10.1021/acs.est.7b05222, 2018b.

19 Li, M., Q. Zhang, J. Kurokawa, J. H. Woo, K. B. He, Z. Lu, T. Ohara, Y. Song, D. G. Streets, G. R. Carmichael, Y.
20 F. Cheng, C. P. Hong, H. Huo, X. J. Jiang, S. C. Kang, F. Liu, H. Su, and Zheng, B.: MIX: a mosaic Asian
21 anthropogenic emission inventory for the MICS-Asia and the HTAP projects, Atmos. Chem. Phys, 17, 935-963,
22 10.5194/acp-17-935-2017, 2017.

23 Liang, J., Horowitz, L. W., Jacob, D. J., Wang, Y., Fiore, A. M., Logan, J. A., Gardner, G. M., and Munger, J. W.:
24 Seasonal budgets of reactive nitrogen species and ozone over the United States, and export fluxes to the global
25 atmosphere,, J. Geophys. Res., 103, 13435–13450,, 1998.

26 Liu, H., Jacob, D. J., Bey, I., and Yantosca, R. M.: Constraints from ^{210}Pb and ^{7}Be on wet deposition and transport in
27 a global three-dimensional chemical tracer model driven by assimilated meteorological fields, J. Geophys. Res., 106,
28 12,109-112,128, 2001.

29 Long, M. S., Keene, W. C., Easter, R. C., Sander, R., Liu, X., Kerkweg, A., and Erickson, D.: Sensitivity of
30 tropospheric chemical composition to halogen-radical chemistry using a fully coupled size-resolved multiphase
31 chemistry-global climate system: halogen distributions, aerosol composition, and sensitivity of climate-relevant
32 gases, Atmos. Chem. Phys, 14, 3397-3425, 10.5194/acp-14-3397-2014, 2014.

33 Lyons, J. R.: Transfer of mass-independent fractioation on ozone to other oxygen-containing molecules in the
34 atmosphere, Geophys. Res. Lett., 28, 3231-3234, 2001.

35 Macintyre, H. L., and Evans, M. J.: Sensitivity of a global model to the uptake of N2O5 by tropospheric aerosol,
36 Atmos. Chem. Phys, 10, 7409-7401, 10.5194/acp-10-7409-2010, 2010.

1   Martin, R. V., Jacob, D. J., Yantosca, R. M., Chin, M., and Ginoux, P.: Global and regional decreases in
2   tropospheric oxidants form photochemical effects of aerosols, J. Geophys. Res., 108, 4097, doi:
3   4010.1029/2002JD002622, 2003.

4   Mauersberger, K., Lämmerzahl, P., and Krankowsky, D.: Stratospheric Ozone Isotope Enrichments—Revisited,
5   Geophys. Res. Lett., 28, 3155-3158, 2001.

6   McCabe, J. R., Boxe, C. S., Colussi, A. J., Hoffmann, M. R., and Thiemens, M. H.: Oxygen isotopic fractionation in
7   the photochemistry of nitrate in water and ice, J. Geophys. Res., 110, D15310, 2005.

8   McCabe, J. R., Savarino, J., Alexander, B., Gong, S., and Thiemens, M. H.: Isotopic constraints on non-
9   photochemical sulfate production in the Arctic winter, Geophys. Res. Lett., 33, L05810, 10.1029/2005GL025164,
10 2006.

11 McCabe, J. R., Thiemens, M. H., and Savarino, J.: A record of ozone variability in South Pole Antarctic snow: Role
12 of nitrate oxygen isotopes, J. Geophys. Res, 112, D12303, doi:10.1029/2006JD007822, 2007.

13 Michalski, G., and Bhattacharya, S. K.: The role of symmetry in the mass independent isotope effect in ozone, Proc.
14 Natl. Acad. Sci., 106, 5493-5496, 2009.

15 Michalski, G. M., Scott, Z., Kabiling, M., and Thiemens, M. H.: First measurements and modeling of $D^{17}O$ in
16 atmospheric nitrate, Geophys. Res. Lett., 30, 1870, doi:1810.1029/2003GL017015, 2003.

17 Morin, S., Savarino, J., Bekki, S., Gong, S., and Bottenheim, J. W.: Signature of Arctic surface ozone depletion
18 events in the isotope anomaly ($D^{17}O$) of atmospheric nitrate, Atmos. Chem. Phys., 6, 6255-6297, 2007.

19 Morin, S., Savarino, J., Frey, M. M., Yan, N., Bekki, S., Bottenheim, J. W., and Martins, J. M. F.: Tracing the
20 Origin and Fate of NO_x in the Arctic Atmosphere Using Stable Isotopes in Nitrate, Science, 322, 730-732,
21 10.1126/science.1161910, 2008.

22 Morin, S., Savarino, J., Frey, M. M., Dominé, F., Jacobi, H.-W., Kaleschke, L., and Martins, J. M. F.:
23 Comprehensive isotopic composition of atmospheric nitrate in the Atlantic Ocean boundary layer from 65S to 79N,
24 J. Geophys. Res, 114, D05303, doi:10.1029/2008JD010696, 2009.

25 Morin, S., Sander, R., and Savarino, J.: Simulation of the diurnal variations of the oxygen isotope anomaly ($D^{17}O$)
26 of reactive atmospheric species, Atmos. Chem. Phys, 11, 3653-3671, doi:10.5194/acp-11-3653-2011, 2011.

27 Müller, J.-F., Peeters, J., and Stavrakou, T.: Fast photolysis of carbonyl nitrates from isoprene,, Atmos. Chem. Phys,
28 14, 2497–2508, 10.5194/acp-14-2497-2014, 2014.

29 Murray, L. T., Jacob, D. J., Logan, J. A., Hudman, R. C., and Koshak, W. J.: Optimized regional and interannual
30 variability of lightning in a global chemical transport model constrained by LIS/OTD satellite data, J. Geophys.
31 Res., 117, D20307, 10.1029/2012JD017934, 2012.

32 Newsome, B., and Evans, M. J.: Impact of uncertainties in inorganic chemical rate constants on tropospheric
33 ocmposition and ozone radiative forcing, Atmos. Chem. Phys, 17, 14333-14352, 10.5194/acp-17-14333-2017, 2017.

34 O'Brien, J., Shepson, P., Muthuramu, K., Hao, C., Niki, H., Hastie, D., Taylor, R., and Roussel, P.: Measurements
35 of alkyl and multifunctional organic nitrates at a rural site in Ontario, J. Geophys. Res., 100, 22795–22804, 1995.

Atmospheric
Chemistry
and Physics
Discussions

1   Parrella, J. P., Jacob, D. J., Liang, Q., Zhang, Y., Mickley, L. J., Miller, B., Evans, M. J., Yang, X., Pyle, J. A.,
2   Theys, N., and Roozendael, M. V.: Tropospheric bromine chemistry: implications for present and pre-industrial
3   ozone and mercury, Atmos. Chem. Phys. , 12, 6723-6740, 10.5194/acp-12-6723-2012, 2012.

4   Paulot, F., Crounse, J. D., Kjaergaard, H. G., Kroll, J. H., Seinfeld, J. H., and Wennberg, P. O.: Isoprene
5   photooxidation: new insights into the production of acids and organic nitrates, Atmos. Chem. Phys., 9, 1479-1501,
6   2009.

7   Ramazan, K. A., Syomin, D., and Finlayson-Pitts, B. J.: The photochemical production of HONO during the
8   heterogeneous hydrolysis of NO_2, Phys. Chem. Chem. Phys., 6, 3836-3843, 10.1039/b402195a, 2004.

9   Reed, C., Evans, M. J., Crilley, L. R., Bloss, W. J., Sherwen, T., Read, K. A., Lee, J. D., and Carpenter, L.: Evidence
10 for renoxification in the tropical marine boundary layer, Atmos. Chem. Phys, 17, 4081-4092, 10.5194/acp-17-4081-
11 2017, 2017.

12 Richter, A., Borrows, J. P., Nub, H., Granier, C., and Niemier, U.: Increase in tropospheric nitrogen dioxide over
13 China observed from space, Nature, 437, 129–132, 10.1038/nature04092, 2005.

14 Rindelaub, J. D., McAvey, K. M., and Shepson, P. B.: The photochemical production of organic nitrates from a-
15 pinene and loss via acid-dependent particle phase hydrolysis,, A`100tm. Env., 193–201,
16 10.1016/j.atmosenv.2014.11.010, 2015.

17 Romer, P. S., Wooldridge, P. J., Crounse, J. D., Kim, M. J., Wennberg, P. O., Dibb, J. E., Scheuer, E., Blake, D. R.,
18 Meinardi, S., Brosius, A. L., Thames, A. B., Miller, D. O., Brune, W. H., Hall, S. R., Ryerson, T. B., and Cohen, R.
19 C.: Constraints on Aerosol Nitrate Photolysis as a Potential Source of HONO and NOx, Environmental Science &
20 Technology, 52, 13738-13746, 10.1021/acs.est.8b03861, 2018.

21 Saiz-Lopez, A., Lamarque, J. F., Kinnison, D. E., Tilmes, S., Ordonez, C., Orlando, J. J., Conley, A. J., Plane, J. M.
22 C., Mahajan, A. S., Sousa Santos, G., ATlas, E. L., Blake, D. R., Sander, S. P., Schauffler, S., Thompson, A. M.,
23 and Brasseur, G. P.: Estimating the climate significance of halogen-driven ozone loss in the tropical marine
24 troposphere, Atmos. Chem. Phys, 12, 3939-3949, 10.5194/acp-12-3939-2012, 2012.

25 Savarino, J., and Thiemens, M. H.: Analytical procedure to determine both $d^{18}O$ and $d^{17}O$ of H_2O_2 in natural water
26 and first measurements, Atmos. Env., 33, 3683-3690, 1999b.

27 Savarino, J., Kaiser, J., Morin, S., Sigman, D. M., and Thiemens, M. H.: Nitrogen and oxygen isotopic constraints
28 on the origin of atmospheric nitrate in coastal Antarctica, Atmos. Chem. Phys., 7, 1925-1945, 2007.

29 Savarino, J., Bhattacharya, S. K., Morin, S., Baroni, M., and Doussin, J.-F.: The $NO+O_3$ reaction: A triple oxygen
30 isotope perspective on the reaction dynamics and atmospheric implications for the transfer of the ozone isotope
31 anomaly, J. Chem. Phys., 128, 194303, 10.1063/1.2917581, 2008.

32 Savarino, J., Morin, S., Erbland, J., Grannec, F., Patey, M., Vicars, W., Alexander, B., and Achterberg, E. P.:
33 Isotopic composition of atmospheric nitrate in a tropical marine boundary layer, PNAS, published ahead of print,
34 doi:10.1073/pnas.1216639110, 2013.

35 Schmidt, J. A., Jacob, D. J., Horowitz, H. M., Hu, L., Sherwen, T., Evans, M. J., Liang, Q., Sulieman, R. M., Oram,
36 D. E., Le Breton, M., Percival, C. J., Wang, S., Dix, B., and Volkamer, R.: Modeling the observed tropospheric BrO
37 background: Importance of multiphase chemistry and implications for ozone, OH, and mercury, J. Geophys. Res.,
38 121, 11,819-811,835, 10.1002/2015JD024229, 2016.

39 Shah, V., Jaeglé, L., Thornton, J. A., Lopez-Hilfiker, F. D., Lee, B. H., Schroder, J. C., Campuzano-Jost, P.,
40 Jimenez, J. L., Guo, H., Sullivan, A. P., Weber, R. J., Green, J. R., Fiddler, M. N., Bililign, S., Campos, T. L., Stell,

M., Weinheimer, A. J., Montzka, D. D., and Brown, S. S.: Chemical feedbacks weaken the wintertime response of particulate sulfate and nitrate to emissions reductions over the eastern United States, Proc. Natl. Acad. Sci., 115, 8110-8115, 10.1073/pnas.1803295115, 2018.

Shao, J., Chen, Q., Wang, Y., Xie, Z., He, P., Sun, Y., Lu, X., Shah, V., Martin, R. V., Philip, S., Song, S., Zhao, Y., Zhang, L., and Alexander, B.: Heterogeneous sulfate aerosol formation mechanisms during wintertime Chinese haze events: Air quality model assessment using observations of sulfate oxygen isotopes in Beijing, in prep, 2018.

Sherwen, T., Schmidt, J. A., Evans, M. J., Carpenter, L. J., Brobmann, K., Eastham, S. D., Jacob, D. J., Dix, B., Koenig, T. K., Sinreich, R., Ortega, I. K., Volkamer, R., Saiz-Lopez, A., Prados-Roman, C., Mahajan, A. S., and Ordonez, C.: Global impacts of tropospheric halogens (Cl, Br, I) on oxidants and composition in GEOS-Chem, Atmos. Chem. Phys, 16, 12239-12271, 10.5194/acp-16-12239-2016, 2016.

Sherwen, T., Evans, M. J., Sommariva, R., Hollis, L. D. J., Ball, S. M., Monks, P. S., Reed, C., Carpenter, L. J., Lee, J. D., Forster, G., Bandy, B., Reeves, C. E., and Bloss, W. J.: Effects of halogens on European air-quality, Faraday Discuss., 200, 75-100, 10.1039/C7FD00026J, 2017.

Singh, H. B., Herlth, D., O'Hara, D., Zahnle, K., Bradshaw, J. D., Sandholm, S. T., Talbot, R., Crutzen, P. J., and Kanakidou, M.: Relationship of Peroxyacetyl nitrate to active and total odd nitrogen at northern high latitudes: Influence of reservoir species on NO_x and O_3, J. Geophys. Res, 97, 16,523-516,530, 1992.

Sofen, E. D., Alexander, B., Steig, E. J., Thiemens, M. H., Kunasek, S. A., Amos, H. M., Schauer, A. J., Hastings, M. G., Bautista, J., Jackson, T. L., Vogel, L. E., McConnell, J. R., Pasteris, D. R., and Saltzman, E. S.: WAIS Divide ice core suggests sustained changes in the atmospheric formation pathways of sulfate and nitrate since the 19th century in the extratropical Southern Hemisphere, Atmos. Chem. Phys. , 14, 5749-5769, 10.5194/acp-14-5749-2014, 2014.

Spataro, F., and Ianniello, A.: Sources of atmospheric nitrous acid: State of the science, current research needs, and future prospects, Journal of the Air and Waste Management Association, 64, 1232-1250, 10.1080/10962247.2014.952846, 2014.

Stettler, M. E. J., Eastham, S., and Barrett, S. R. H.: Air quality and public health impacts of UK airports. Part I: Emissions, Atm. Env., 45, 5415-5424, 10.1016/j.atmosenv.2011.07.012, 2011.

Tan, F., Tong, S., Jing, B., Hou, S., Liu, Q., Li, K., Zhang, Y., and Ge, M.: Heterogeneous reactions of NO_2 with $CaCO_3$–$(NH_4)_2SO_4$ mixtures at different relative humidities, Atmos. Chem. Phys, 16, 8081-8093, 10.5194/acp-16-8081-2016, 2016.

Tong, S. R., Hou, S. Q., Zhang, Y., Chu, B. W., Liu, Y. C., He, H., Zhao, P. S., and Ge, M. F.: Exploring the nitrous acid (HONO) formation mechanism in winter Beijing: direct emissions and heterogeneous production in urban and suburban areas, Faraday Discuss., 189, 213-230, 10.1039/c5fd00163c, 2016.

Vicars, W., and Savarino, J.: Quantitative constraints on the ^{17}O-excess ($D^{17}O$) signature of surface ozone: Ambient measurements from 50°N to 50°S using the nitrite-coated filter technique, Geochem. Cosmochem. Acta, 135, 270-287, 10.1016/j.gca.2014.03.023, 2014.

Vicars, W. C., Bhattacharya, S. K., Erbland, J., and Savarino, J.: Measurement of the 17O-excess ($D^{17}O$) of tropospheric ozone using a nitrite-coated filter, Rapid Commun. Mass Spectrom., 26, 1219-1231, 10.1002/rcm.6218, 2012.

Vinken, G. C. M., Boersma, K. F., Jacob, D. J., and Meijer, E. W.: Accounting for non-linear chemistry of ship plumes in the GEOS-Chem global chemistry transport model, Atmos. Chem. Phys, 11, 11707-11722, 10.5194/acp-11-11707-2011, 2011.

Atmospheric
Chemistry
and Physics
Discussions

1 von Glasow, R., and Crutzen, P. J.: Model study of multiphase DMS oxidation with a focus on halogens, Atmos.
2 Chem. Phys., 4, 589-608, 2004.

3 Wang, J. Q., Zhang, X. S., Guo, J., Wang, Z. W., and Zhang, M. G.: Observation of nitrous acid (HONO) in Beijing,
4 China: Seasonal variation, nocturnal formation and daytime budget, Science of the Total Environment, 587,
5 10.1016/j.scitotenv.2017.02.159, 2017.

6 Wang, X., Jacob, D. J., Eastham, S., Sulprizio, M., Zhu, L., Chen, Q., Alexander, B., Sherwen, T., Evans, M. J., Lee,
7 B. H., Haskins, J., Lopez-Hilfiker, F. D., Thornton, J. A., Huey, L. G., and Liao, H.: The role of chlorine in
8 tropospheric chemistry, Atmos. Chem. Phys. Discuss., 10.5194/acp-2018-1088, 2018.

9 Wang, Y. H., Jacob, D. J., and Logan, J. A.: Global simulation of tropospheric O_3-NO_x hydrocarbon chemistry 1.
10 Model formulation, J. Geophys. Res., 103, 10,713-710,725, 1998.

11 Xu, L., Guo, H., Boyd, C. M., Klein, M., Bougiatioti, A., Cerully, K. M., Hite, J. R., Isaacman-VanWertz, G.,
12 Kreisberg, N. M., Knote, C., Olson, K., Koss, A., Goldstein, A. H., Hering, S. V., de Gouw, J., Baumann, K., Lee,
13 S.-H., Nenes, A., Weber, R. J., and Ng, N. L.: Effects of anthropogenic emissions on aerosol formation from
14 isoprene and monoterpenes in the southeastern United States, Proc. Natl. Acad. Sci., 112, 37–42,
15 10.1073/pnas.1417609112, 2015.

16 Xu, W., Kuang, Y., Zhao, C., Tao, J., Zhao, G., Bian, Y., Yu, Y., Shen, C., Liang, L., and Zhang, G.: NH3-promoted
17 hydrolysis of NO2 induces explosive 1 growth in HONO, Atmos. Chem. Phys. Discuss.,
18 https://doi.org/10.5194/acp-2018-996, 2018.

19 Yabushita, A., Enami, S., Sakamoto, Y., Kawasaki, M., Hoffman, M. R., and Colussi, A. J.: Anion-Catalyzed
20 Dissolution of NO2 on Aqueous Microdroplets, J. Phys. Chem. A Lett., 113, 4844–4848, 10.1021/jp900685f, 2009.

21 Ye, C., Zhou, X., Pu, D., Stutz, J., Festa, J., Spolaor, M., Tsai, C., Cantrell, C., Mauldin Iii, R. L., Campos, T.,
22 Weinheimer, A., Hornbrook, R. S., Apel, E., Guenther, A., Kaser, L., Yuan, B., Karl, T., Haggerty, J., Hall, S.,
23 Ullmann, K., Smith, J. N., Ortega, J., and Knote, C.: Rapid cycling of reactive nitrogen in the marine boundary
24 layer, Nature, 532, 489-491, 10.1038/nature17195, 2016.

25 Ye, C., Zhou, X., Pu, D., Stutz, J., Festa, J., Spolaor, M., Tsai, C., Cantrell, C., Mauldin III, R. L., Weinheimer, A.,
26 Hornbrook, R. S., Apel, E. C., Guenther, A., Kaser, L., Yuan, B., Karl, T., Haggerty, J., Hall, S., Ullmann, K.,
27 Smith, J., and Ortega, J.: Tropospheric HONO distribution and chemistry in the southeastern US, Atmos. Chem.
28 Phys, 18, 9107-9120, 10.5194/acp-18-9107-2018, 2018.

29 Zare, A., Romer, P. S., Nguyen, T., Keutsch, F. N., Skog, K., and Cohen, R. C.: A comprehensive organic nitrate
30 chemistry: insights into the lifetime of atmospheric organic nitrates, Atmos. Chem. Phys. Discuss., 10.5194/acp-
31 2018-530, 2018.

32 Zhang, L., Gong, S., Padro, J., and Barrie, L.: A size-segregated particle dry deposition scheme for an atmosopheric
33 aerosol module, Atmos. Env., 35, 549-560, 2001.

34

35

36

37

Atmospheric
Chemistry
and Physics
Discussions

1   **Table 1.** Calculated $\Delta^{17}O$(nitrate) in the model for each nitrate production pathway (X = Br, Cl,

2   and I; HC = hydrocarbon; MTN = monoterpene; ISOP = isoprene; $\Delta^{17}O(O_3^*) = 39‰$).

3

		Nitrate formation pathway	Δ^{17}O(nitrate)
		Gas-phase reactions	
R1		NO_2 + OH	$\frac{2}{3} A\Delta^{17}O(O_3^*)$
R2		NO_3 + HC	$\left(\frac{2}{3}A + \frac{1}{3}\right)\Delta^{17}O(O_3^*)$
R3		NO + HO_2	$\frac{1}{3}A\Delta^{17}O(O_3^*)$
		Aerosol uptake from the gas-phase followed by hydrolysis	
R4		N_2O_5 + $H_2O_{(aq)}$	$\left(\frac{2}{3}A + \frac{1}{6}\right)\Delta^{17}O(O_3^*)$
R5		N_2O_5 + Cl^-(aq)	$\left(\frac{2}{3}A + \frac{1}{3}\right)\Delta^{17}O(O_3^*)$
R6		XNO_3 + $H_2O_{(aq)}$	$\left(\frac{2}{3}A + \frac{1}{3}\right)\Delta^{17}O(O_3^*)$
R7		NO_2 + $H_2O_{(aq)}$	$\frac{2}{3}A\Delta^{17}O(O_3^*)$
R8		NO_3 + $H_2O_{(aq)}$	$\left(\frac{2}{3}A + \frac{1}{3}\right)\Delta^{17}O(O_3^*)$
R9		$RONO_2$ + $H_2O_{(aq)}$ (where $RONO_2$ is from NO + RO_2)	$\frac{1}{3}A\Delta^{17}O(O_3^*)$
R10		$RONO_2$ + $H_2O_{(aq)}$ (where $RONO_2$ is from NO_3 + MTN/ISOP)	$\left(\frac{2}{3}A + \frac{1}{3}\right)\Delta^{17}O(O_3^*)$

4

5

6

7

8

9

10
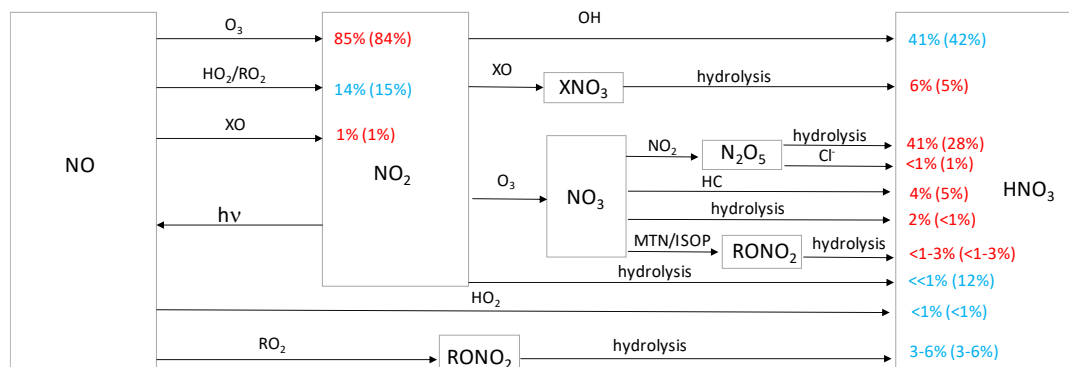
Figure 1. Simplified HNO_3 formation in the model. Numbers show the global, annual mean percent contribution to NO_2 and HNO_3 formation in the troposphere below 1 km for the "cloud chem" ("standard") simulation. Red indicates reactions leading to high $D^{17}O$ values, blue indicates reactions leading to low $D^{17}O$ values. $HO_2 = HO_2+RO_2$; X = Br+Cl+I; HC = hydrocarbons; MTN = monoterpenes; ISOP = isoprene.
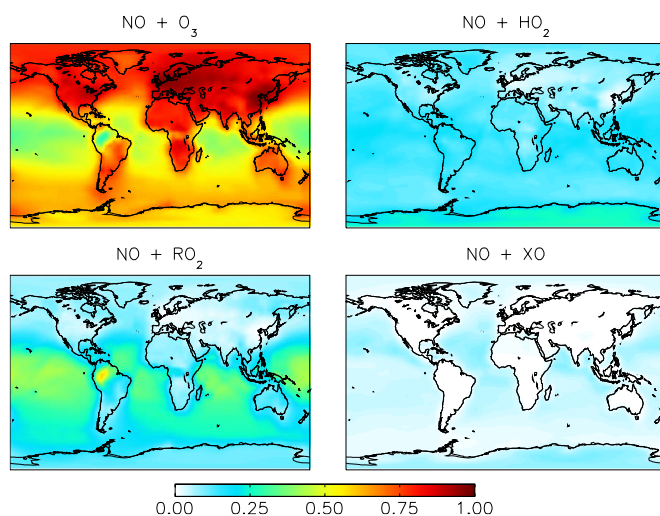
Figure 2. Annual-mean fraction of NO_2 formation from the oxidation of NO in the troposphere below 1 km altitude in the "cloud chemistry" model.
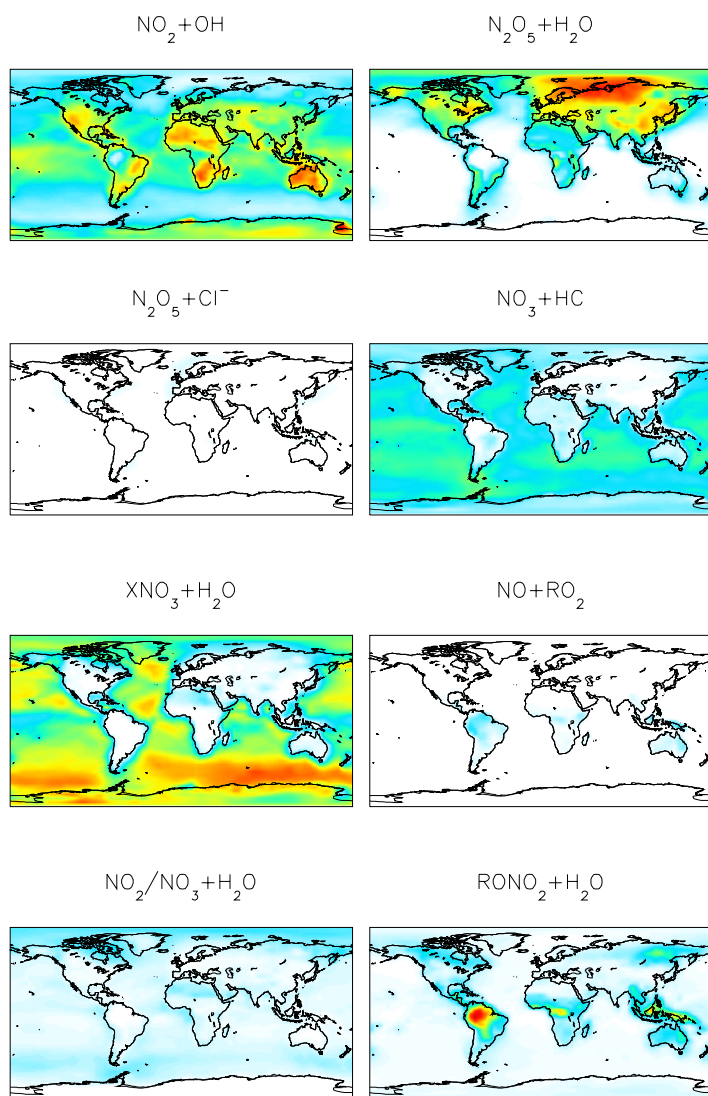
Figure 3. Annual-mean fraction of HNO_3 formation from the oxidation of NO_x in the troposphere below 1 km altitude in the "cloud chemistry" model.

1

2
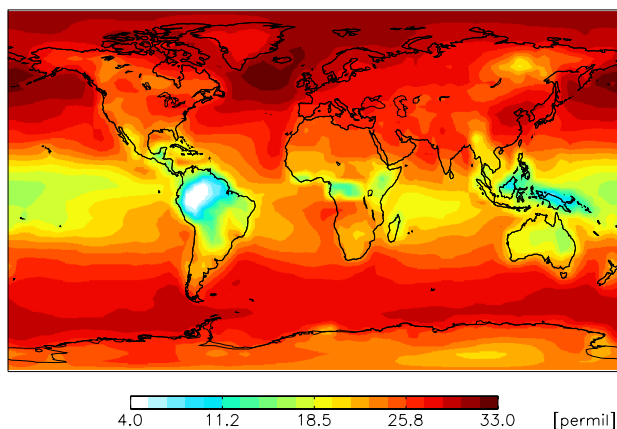
Figure 4. Modeled, annual-mean $\Delta^{17}O$(nitrate) below 1 km altitude for the "cloud chemistry" model.

4

5

6
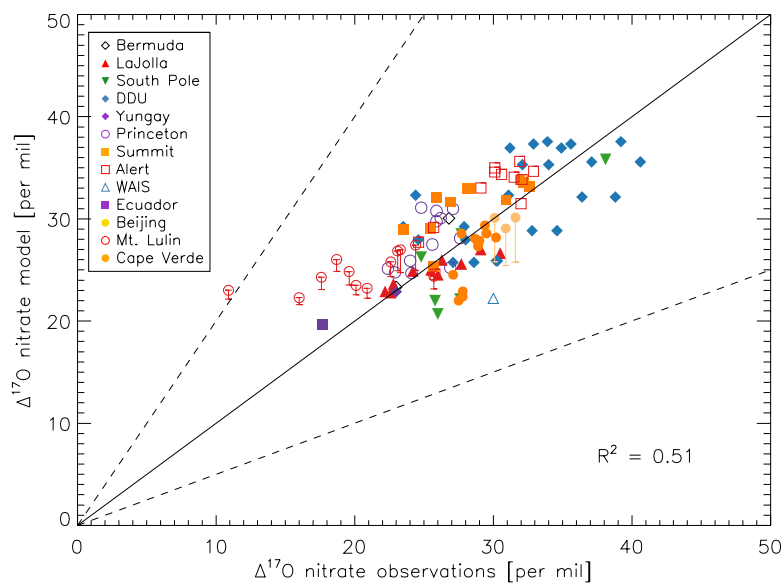
Figure 5. Comparison of monthly-mean modeled ("cloud chemistry") and observed $D^{17}O$(nitrate) at locations where there are enough observations to calculate a monthly mean. References for the observations are in the text. The error bars represent different assumptions for calculated modeled A values for nighttime reactions as described in the text. Error bars for Beijing and Mt. Lulin reflect the range of possible modeled A values for nighttime reactions as described in the text.

12

Atmospheric
Chemistry
and Physics
Discussions
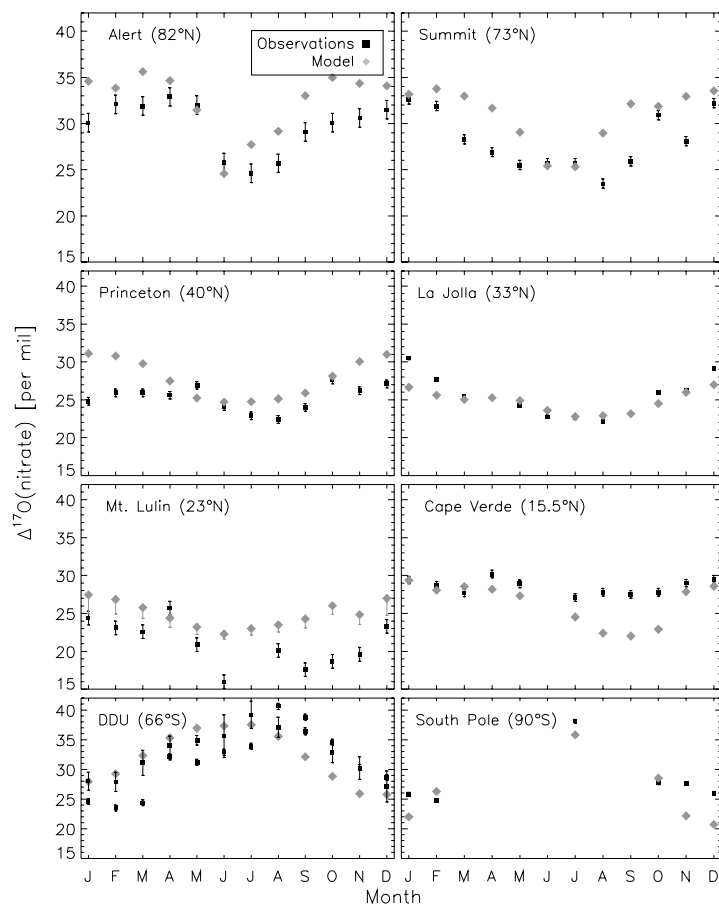
1

2   **Figure 6.** Comparison of monthly-mean modeled ("cloud chemistry") and observed $\mathrm{D}^{17}\mathrm{O}$(nitrate). Error

3   bars for Mt. Lulin reflect the range of possible modeled A values for nighttime reactions as described in

4   the text.

5

6

7

8

9

10

11

12

13
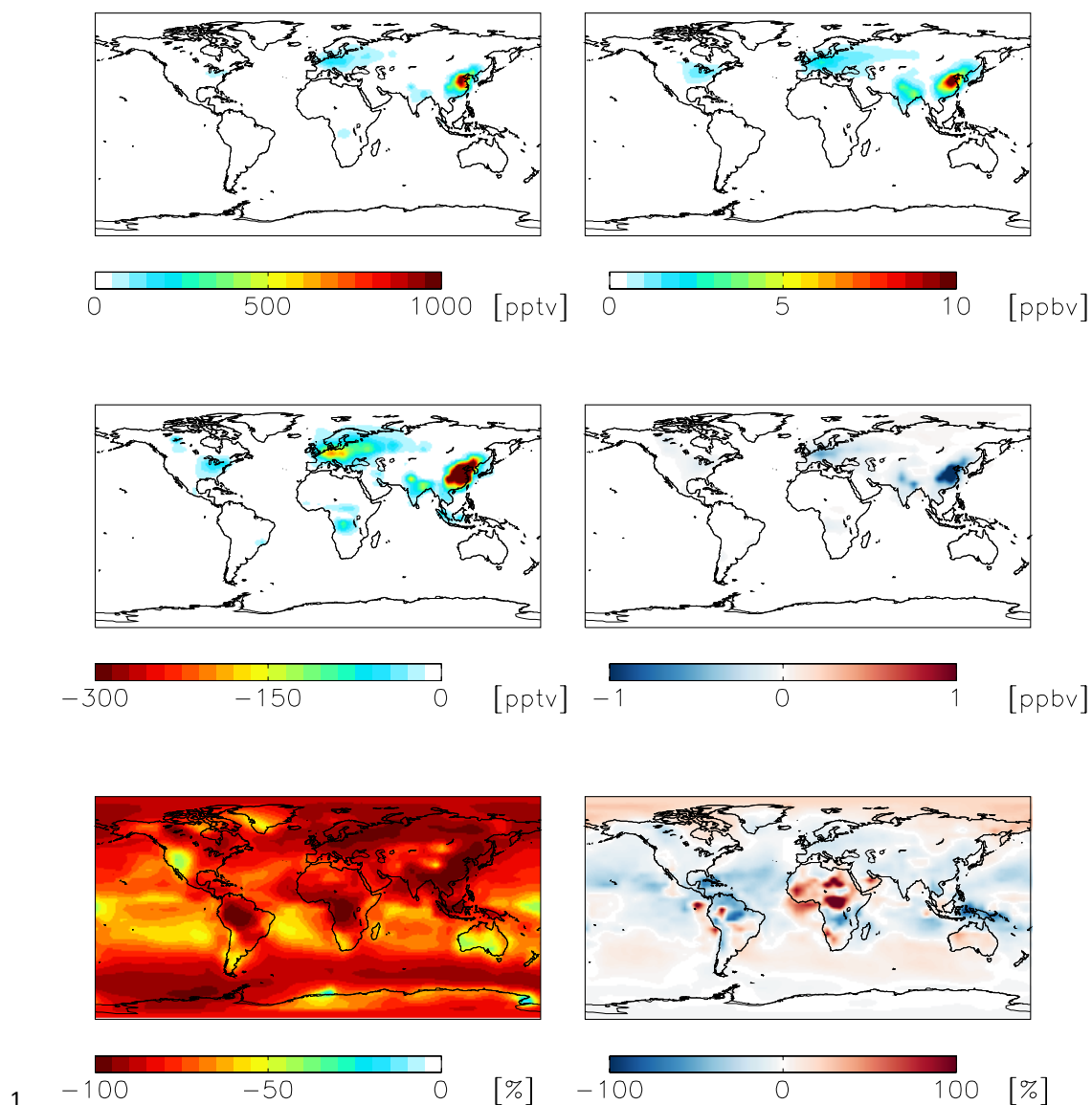
1

2

3   **Figure 7.** Modeled annual-mean HONO (left) and fine-mode nitrate (right) concentrations below 1 km
4   altitude in the "standard" simulation (top) with $g_{NO2} = 10^{-4}$ for NO_2 hydrolysis. Absolute (middle) and
5   relative (bottom) change in concentrations below 1 km altitude between the "standard" model and the
6   model simulation with $g_{NO2} = 10^{-7}$. Negative numbers represent a decrease relative to the standard
7   simulation.
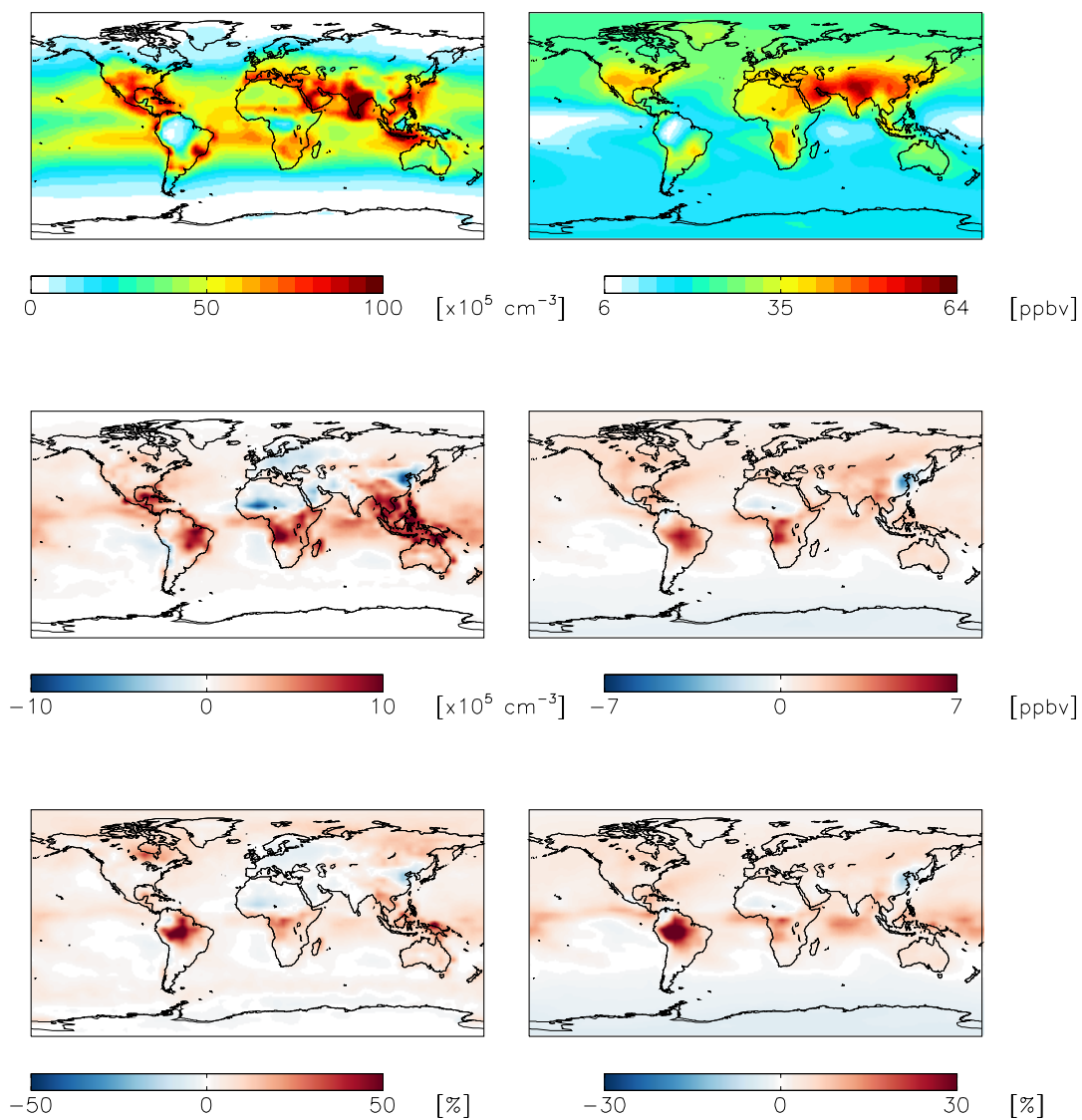
Figure 8. Same as Figure 7 except for OH (left) and ozone (right).

Atmospheric
Chemistry
and Physics
Discussions

1
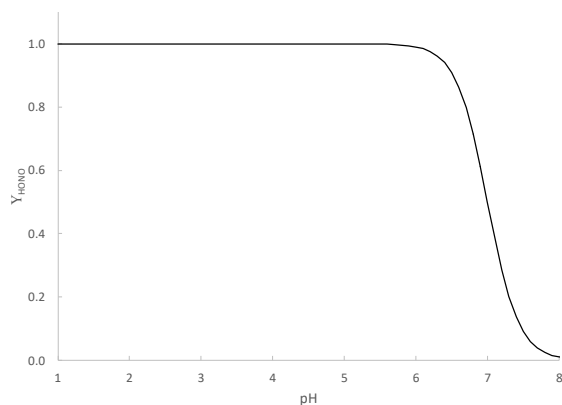
Figure 9. Calculated yield of HONO from the heterogeneous reaction of NO_2 on aerosol surfaces as a
function of pH.
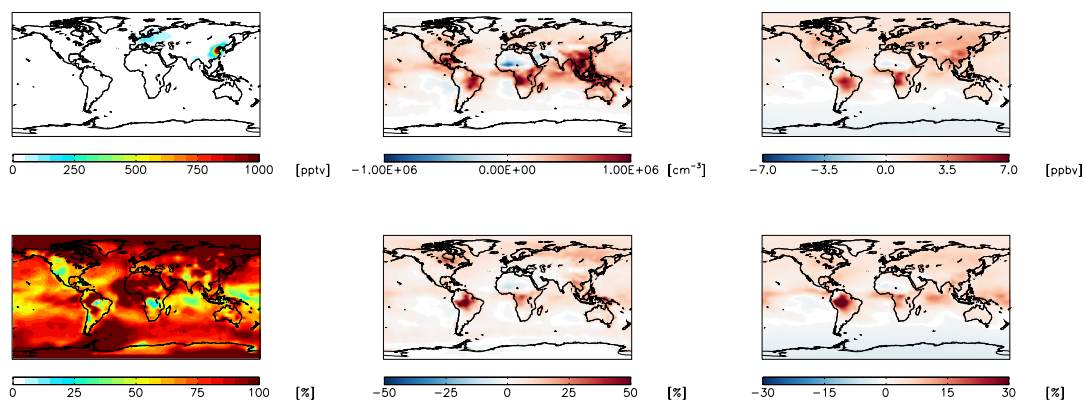
Figure 10. Absolute (top) and relative (bottom) change in HONO (left), OH (middle), and ozone (right)
concentrations below 1 km altitude between the "standard" model and the model simulation with an
acidity-dependent yield from NO_2 hydrolysis. Positive numbers represent an increase relative to the
"standard" simulation.

1
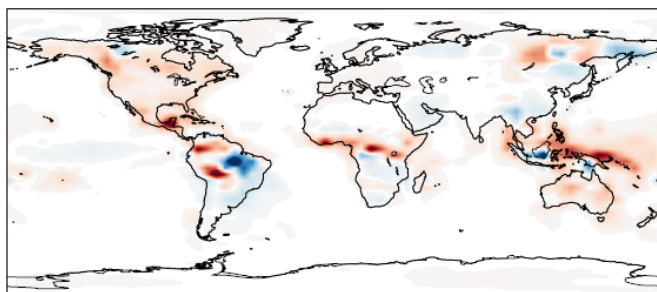
Figure 11. Modeled annual-mean difference in the fractional production rate of HNO$_3$ from the
hydrolysis of organic nitrate below 1 km attitude in the year 2015 relative to 2000 (2015 − 2000).

2

3

4

5